UNIVERSITY OF CALIFORNIA

Santa Barbara

Mathematical Approaches to Understanding Mammalian Circadian Rhythms

by

Peter C. St. John

Committee in charge:

Professor Francis J. Doyle III, Chair

Professor Samir Mitragotri

Professor Michelle A. O'Malley

Professor Linda R. Petzold

June 2015

The dissertation of Peter C. St. John is approved.

Samir Mitragotri	Date
Michelle A. O'Malley	Date
Linda R. Petzold	Date
Francis J. Doyle III, Committee Chair	Date

Mathematical Approaches to Understanding Mammalian Circadian Rhythms

Peter C. St. John

Acknowledgement

Hello, here is some text without a meaning. This text should show what a printed text will look like at this place. If you read this text, you will get no information. Really? Is there no information? Is there a difference between this text and some nonsense like “Huardest gefburn”? Kjift – not at all! A blind text like this gives you information about the selected font, how the letters are written and an impression of the look. This text should contain all letters of the alphabet and it should be written in of the original language. There is no need for special content, but the length of words should match the language.

This is the second paragraph. Hello, here is some text without a meaning. This text should show what a printed text will look like at this place. If you read this text, you will get no information. Really? Is there no information? Is there a difference between this text and some nonsense like “Huardest gefburn”? Kjift – not at all! A blind text like this gives you information about the selected font, how the letters are written and an impression of the look. This text should contain all letters of the alphabet and it should be written in of the original language. There is no need for special content, but the length of words should match the language.

And after the second paragraph follows the third paragraph. Hello, here is some text without a meaning. This text should show what a printed text will look like at this place. If you read this text, you will get no information. Really? Is there no information? Is there a difference between this text and some nonsense like “Huardest gefburn”? Kjift – not at all! A blind text like this gives you information about the selected font, how the letters are written and an impression of the look. This text should contain all letters of the alphabet and it should be written in of the original language. There is no need for special content, but the length of words should match the language.

After this fourth paragraph, we start a new paragraph sequence. Hello, here is

some text without a meaning. This text should show what a printed text will look like at this place. If you read this text, you will get no information. Really? Is there no information? Is there a difference between this text and some nonsense like “Huardest gefburn”? Kjift – not at all! A blind text like this gives you information about the selected font, how the letters are written and an impression of the look. This text should contain all letters of the alphabet and it should be written in of the original language. There is no need for special content, but the length of words should match the language.

Hello, here is some text without a meaning. This text should show what a printed text will look like at this place. If you read this text, you will get no information. Really? Is there no information? Is there a difference between this text and some nonsense like “Huardest gefburn”? Kjift – not at all! A blind text like this gives you information about the selected font, how the letters are written and an impression of the look. This text should contain all letters of the alphabet and it should be written in of the original language. There is no need for special content, but the length of words should match the language.

Vita of Peter C. St. John

Contact Information

Department of Chemical Engineering
University of California, Santa Barbara
Santa Barbara, CA 93106-5080

Phone: (508) 494-2474
E-mail: pstjohn@engineering.ucsb.edu
Office: Engineering II, Rm. 1508

Education

University of California, Santa Barbara — **September 2010 - present**
Ph.D. Candidate, Department of Chemical Engineering — Santa Barbara, California

Tufts University — **September 2006 - May 2010**
BS, Chemical and Biological Engineering — Medford, Massachusetts

Honors and Awards

CAST Student Travel Grant **September 2014**
Society for Research on Biological Rhythms (SRBR) Research Merit Award **June 2014**
Best Poster, Center for Chronobiology Symposium, UCSD **February 2014**
1st Place, SRBR Logo Competition **January 2014**
Mitsubishi Chemical Fellowship Recipient **2012-2015**
UCSB Scienceline 2011-2012 Life Science Outstanding Answerer **June 2012**
National Science Foundation GRFP Honorable Mention **April 2011**
Class of 1947 Victor Prather Prize **May 2010**
Max Tischler Prize Scholarship **May 2009**
Elected to Tau Beta Pi **September 2008**

Publications

St. John, P.C., Taylor, S.R., Abel, J.H., and F.J. Doyle III. Amplitude metrics for cellular circadian bioluminescence reporters (2014) *Biophysical Journal*, 107 (11) pp. 2712-2722

St. John, P.C., Hirota, T., Kay, S.A. and F.J. Doyle III. Spatiotemporal separation of PER and CRY posttranslational regulation in the mammalian circadian clock (2014) *PNAS*, 111 (5) pp. 2040-2045.

Yang, R., Rodriguez-Fernandez, M., **St. John, P.C.,** and F.J. Doyle III. Chapter 8 – Systems Biology (2014) In E. Carson and C. Cobelli (Eds.) *Modelling Methodology for Physiology and Medicine, 2nd Edition*, pp. 159-187.

St. John, P.C., and F.J. Doyle III. Estimating confidence intervals in predicted responses for oscillatory biological models (2013) *BMC Systems Biology* 7:71.

Hirota, T., Lee, J.W., **St. John, P.C.**, Sawa, M., Iwaisako, K., Noguchi, T., Pongsawakul, P.Y., Sonntag, T., Welsh, D.K., Brenner, D.A., Doyle, F.J. III, Schultz, P.G., Kay, S.A., Identification of small molecule activators of cryptochrome (2012) *Science*, 337 (6098) pp. 1094-1097.

Murphy A.R., **St. John P.C.**, Kaplan D.L. Modification of silk fibroin using diazonium coupling chemistry and the effects on hMSC proliferation and differentiation (2008) *Biomaterials*, 29 (19), pp. 2829-2838.

Contributed Talks

St. John, P.C., and F.J. Doyle III. November 2014. Development of Amplitude Response Curves for Single-Cell and Population-Level Circadian Systems. *To be presented* at the 2014 AIChE Annual Meeting, Atlanta, GA

St. John, P.C., and F.J. Doyle III. June 2014. Amplitude metrics for uncoupled cellular circadian bioluminescence reporters. Presented at the Society for Research on Biological Rhythms Meeting, Big Sky, MT.

St. John, P.C., and F.J. Doyle III. October 2012. Cryptochrome balancing for period control: mathematical insights into circadian clock design. Presented at the Model-based Analysis and Control of Cellular Processes Workshop, Purdue University, West Lafayette, IN.

Poster Presentations

St. John, P.C., and F.J. Doyle III. February 2014. Spatiotemporal separation of PER and CRY post-translation regulation. Presented at the UCSD Center for Chronobiology Symposium, La Jolla, CA.

St. John, P.C., T. Hirota, S.A. Kay, and F.J. Doyle III. July 2013. Estimating confidence intervals in model predictions to determine plausible mechanisms for small molecule modifiers. Presented at the Chronobiology Gordon Research Conference, Newport, RI.

St. John, P.C., and F.J. Doyle III. February 2013. Predictive confidence intervals from mathematical circadian models. Presented at the UCSD Center for Chronobiology Symposium, La Jolla, CA.

St. John, P.C., T. Hirota, S. Kay, and F.J. Doyle III. May 2012. Cryptochrome balancing for period control. Presented at the Meeting of the Society for Research on Biological Rhythms, Destin, FL.

St. John, P.C., and F.J. Doyle III. February 2012. Perturbation analysis of circadian clock degradation. Presented at the UCSD Center for Chronobiology Symposium, La Jolla, CA.

St. John, P.C., M. Rodriguez-Fernandez, and F.J. Doyle III. June 2011. Advanced global optimization and sensitivity techniques for analyzing deterministic circadian models. Presented at the 12th Annual UC Systemwide Bioengineering Symposium, Santa Barbara, CA.

Seminars

St. John, P.C. May 2013. Sensitivity analysis in the study of mammalian circadian rhythms. Presented at the UCSB NSF-IGERT systems biology seminar series, Santa Barbara, CA.

Research Experience

University of California, Santa Barbara **September 2010 - present**
Ph.D. Candidate Santa Barbara, California
Computational analysis of the mammalian circadian clock, with a focus on elucidating the functional design consequences of the underlying genetic regulatory network.
Advisor: Francis J. Doyle III
Department: Chemical Engineering

Tufts University **September 2009 - May 2010**
Senior Honors Thesis Medford, Massachusetts
Catalytic Hydrodechlorination of 2-Chlorophenol using Viral-templated Palladium Nanoparticles
Advisor: Hyunmin Yi
Department: Chemical and Biological Engineering

University of California, Los Angeles **June 2009 - August 2009**
UCLA NanoCER Program (NSF REU) Los Angeles, California
Encapsulation Efficiencies and Release Rates from Water-in-Oil-in-Water Nanoemul-

sions
Advisor: Timothy Deming
Department: Bioengineering

Tufts University **June 2008 - August 2008**
Tufts Summer Scholars Medford, Massachusetts
Hydrodechlorination of 2-Chlorophenol with Palladium Nanoparticles on Genetically Modified Tobacco Mosaic Virus Scaffolds
Advisor: Hyunmin Yi
Department: Chemical and Biological Engineering

Tufts University **October 2007 - May 2008**
Undergraduate Research Credit Medford, Massachusetts
Chemically Modified Silk Fibroin Based Scaffolds for Bone Tissue Engineering
Advisor: David Kaplan
Department: Biomedical Engineering

Teaching Experience

University of California, Santa Barbara **January 2013 - December 2013**
Teaching Assistant, ChE132c Santa Barbara, California
Helped teach undergraduate statistics for two subsequent years: gave three lectures, held office hours and review sessions, and graded homeworks.

University of California, Santa Barbara **March 2012 - June 2012**
Teaching Assistant, ChE180a Santa Barbara, California
Designed and ran experiments for the junior laboratory course. Also helped in grading student reports.

Community Involvement

Peer Review **January 2014-present**
Reviewer for Biophysical Journal; IEEE Control Systems Society Conference; 21st International Symposium on Mathematical Theory of Networks and Systems

Scienceline “Ask A Scientist" **December 2010 - present**
Answers science and engineering questions posed by students and teachers from local K-12 schools.
Website: www.scienceline.ucsb.edu

UCSB Discover Engineering Weekend **May 2011**
Helped organize and run a weekend for local high school students to learn basic en-

gineering principles and apply their knowledge to build miniature alternative energy cars.

Mentoring Experience

Amanda Luan, Undergraduate Student, ICB SSB URAP **June 2014 - December 2014**
Lukas Widmer, Masters Student, ETH Zurich **April 2012 - February 2013**
Andrew Barisser, Rotation Student, BMSE UCSB **September 2012 - December 2012**

Abstract

This is the second paragraph. Hello, here is some text without a meaning. This text should show what a printed text will look like at this place. If you read this text, you will get no information. Really? Is there no information? Is there a difference between this text and some nonsense like “Huardest gefburn”? Kjift – not at all! A blind text like this gives you information about the selected font, how the letters are written and an impression of the look. This text should contain all letters of the alphabet and it should be written in of the original language. There is no need for special content, but the length of words should match the language.

And after the second paragraph follows the third paragraph. Hello, here is some text without a meaning. This text should show what a printed text will look like at this place. If you read this text, you will get no information. Really? Is there no information? Is there a difference between this text and some nonsense like “Huardest gefburn”? Kjift – not at all! A blind text like this gives you information about the selected font, how the letters are written and an impression of the look. This text should contain all letters of the alphabet and it should be written in of the original language. There is no need for special content, but the length of words should match the language.

After this fourth paragraph, we start a new paragraph sequence. Hello, here is some text without a meaning. This text should show what a printed text will look like at this place. If you read this text, you will get no information. Really? Is there no information? Is there a difference between this text and some nonsense like “Huardest gefburn”? Kjift – not at all! A blind text like this gives you information about the selected font, how the letters are written and an impression of the look. This text should contain all letters of the alphabet and it should be written in of the original language. There is no need for special content, but the length of words should match the language.

Hello, here is some text without a meaning. This text should show what a printed text will look like at this place. If you read this text, you will get no information. Really? Is there no information? Is there a difference between this text and some nonsense like “Huardest gefburn”? Kjift – not at all! A blind text like this gives you information about the selected font, how the letters are written and an impression of the look. This text should contain all letters of the alphabet and it should be written in of the original language. There is no need for special content, but the length of words should match the language.

This is the second paragraph. Hello, here is some text without a meaning. This text should show what a printed text will look like at this place. If you read this text, you will get no information. Really? Is there no information? Is there a difference between this text and some nonsense like “Huardest gefburn”? Kjift – not at all! A blind text like this gives you information about the selected font, how the letters are written and an impression of the look. This text should contain all letters of the alphabet and it should be written in of the original language. There is no need for special content, but the length of words should match the language.

Contents

List of Figures

Chapter 1

Introduction

1.1 Biological background

Systems biology is a multidisciplinary field, drawing from biology, mathematics, and computer science. In this section, I first provide a background on the biology of circadian rhythms, followed by previous literature on computational modeling.

Ecological competition drives species to optimize their survival and reproduction in a particular environmental niche. Aspects of their environment, including temperature, resource availability, and sunlight are all important factors in determining an individual's success.

In nearly all environments, however, these factors vary greatly from hour to hour and month to month. While food or sunlight might be plentiful during daylight hours, the threat of predators might peak as well. Fortunately, while these critical parameters undergo sharp changes, they do so with a predictable and repeatable schedule. It is not surprising that, in optimizing their survival in an oscillating environment, species have developed a means to predict changes and to ready themselves for the correct behavior.

Biological rhythms are classified as *circadian* if they display a number of defining

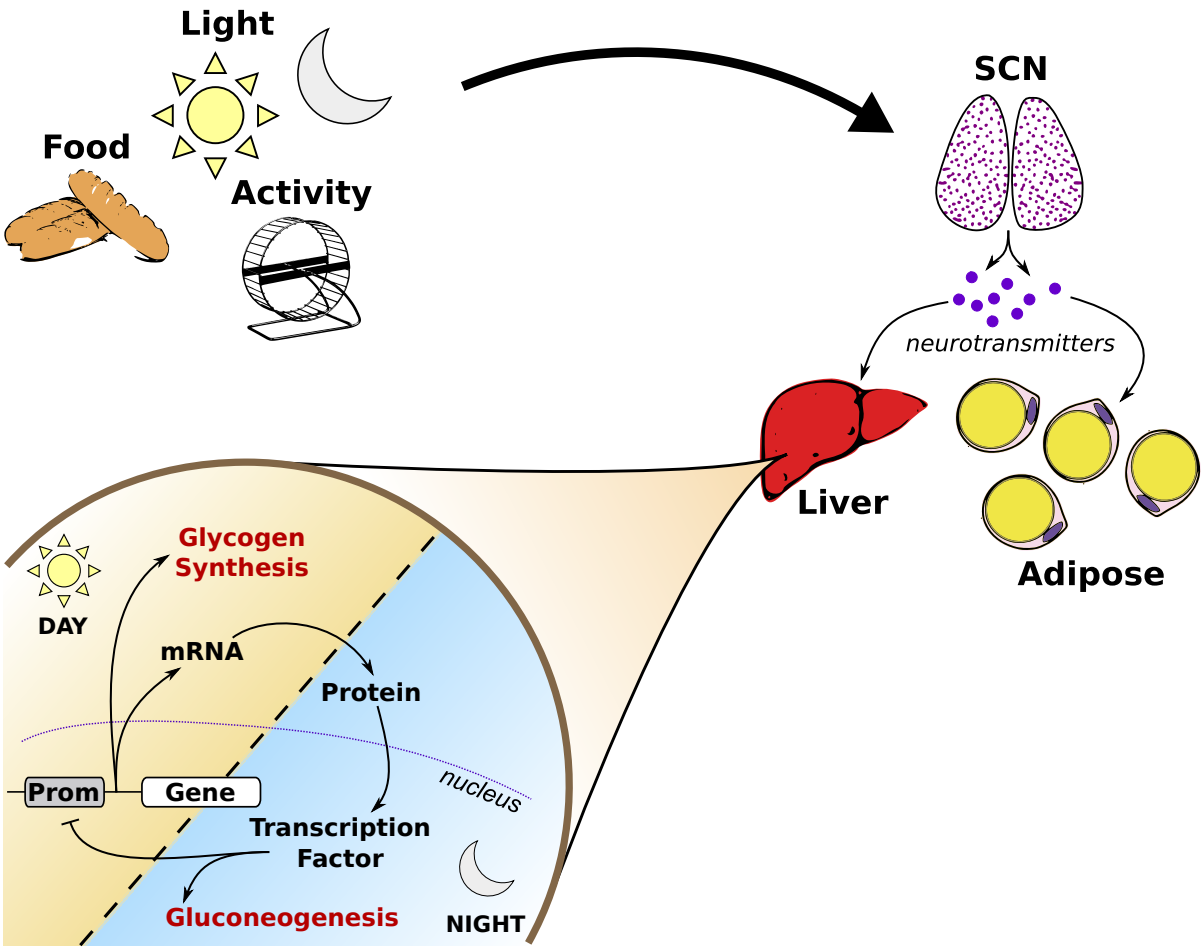

Figure 1.1: A biological feed forward controller. Circadian rhythms

characteristics:

- They are *endogenous*, meaning they continue to oscillate even when the organism is isolated from its environment
- They are temperature compensated, maintaining a consistent period for moderate changes in average temperature
- They are *entrainable*, meaning they can adjust their phase and period in response to a changing in environmental signal
- They oscillate with a roughly 24 hour period [1].

1.1.1 Evolutionary history

Hello, here is some text without a meaning. This text should show what a printed text will look like at this place. If you read this text, you will get no information. Really? Is there no information? Is there a difference between this text and some nonsense like “Huardest gefburn”? Kjift – not at all! A blind text like this gives you information about the selected font, how the letters are written and an impression of the look. This text should contain all letters of the alphabet and it should be written in of the original language. There is no need for special content, but the length of words should match the language.

1.1.2 Mechanisms of gene regulation

Hello, here is some text without a meaning. This text should show what a printed text will look like at this place. If you read this text, you will get no information. Really? Is there no information? Is there a difference between this text and some nonsense like “Huardest gefburn”? Kjift – not at all! A blind text like this gives you information about the selected font, how the letters are written and an impression of the look. This text should contain all letters of the alphabet and it should be written in of the original language. There is no need for special content, but the length of words should match the language.

1.1.3 Mammalian genetic circuit

Hello, here is some text without a meaning. This text should show what a printed text will look like at this place. If you read this text, you will get no information. Really? Is there no information? Is there a difference between this text and some nonsense like “Huardest gefburn”? Kjift – not at all! A blind text like this gives you information about the selected font, how the letters are written and an impression of

the look. This text should contain all letters of the alphabet and it should be written in of the original language. There is no need for special content, but the length of words should match the language.

1.2 Mathematical modeling

Hello, here is some text without a meaning. This text should show what a printed text will look like at this place. If you read this text, you will get no information. Really? Is there no information? Is there a difference between this text and some nonsense like “Huardest gefburn”? Kjift – not at all! A blind text like this gives you information about the selected font, how the letters are written and an impression of the look. This text should contain all letters of the alphabet and it should be written in of the original language. There is no need for special content, but the length of words should match the language.

1.2.1 Overview of kinetic ODE models

Hello, here is some text without a meaning. This text should show what a printed text will look like at this place. If you read this text, you will get no information. Really? Is there no information? Is there a difference between this text and some nonsense like “Huardest gefburn”? Kjift – not at all! A blind text like this gives you information about the selected font, how the letters are written and an impression of the look. This text should contain all letters of the alphabet and it should be written in of the original language. There is no need for special content, but the length of words should match the language.

Spectrum of modeling methods (detail vs. scope)

Hello, here is some text without a meaning. This text should show what a printed text will look like at this place. If you read this text, you will get no information. Really? Is there no information? Is there a difference between this text and some nonsense like “Huardest gefburn”? Kjift – not at all! A blind text like this gives you information about the selected font, how the letters are written and an impression of the look. This text should contain all letters of the alphabet and it should be written in of the original language. There is no need for special content, but the length of words should match the language.

1.2.2 Basic terms and assumptions

Hello, here is some text without a meaning. This text should show what a printed text will look like at this place. If you read this text, you will get no information. Really? Is there no information? Is there a difference between this text and some nonsense like “Huardest gefburn”? Kjift – not at all! A blind text like this gives you information about the selected font, how the letters are written and an impression of the look. This text should contain all letters of the alphabet and it should be written in of the original language. There is no need for special content, but the length of words should match the language.

Mass action

Hello, here is some text without a meaning. This text should show what a printed text will look like at this place. If you read this text, you will get no information. Really? Is there no information? Is there a difference between this text and some nonsense like “Huardest gefburn”? Kjift – not at all! A blind text like this gives you information about the selected font, how the letters are written and an impression of

the look. This text should contain all letters of the alphabet and it should be written in of the original language. There is no need for special content, but the length of words should match the language.

Michealis-Menten

Hello, here is some text without a meaning. This text should show what a printed text will look like at this place. If you read this text, you will get no information. Really? Is there no information? Is there a difference between this text and some nonsense like "Huardest gefburn"? Kjift – not at all! A blind text like this gives you information about the selected font, how the letters are written and an impression of the look. This text should contain all letters of the alphabet and it should be written in of the original language. There is no need for special content, but the length of words should match the language.

Hill-type

Hello, here is some text without a meaning. This text should show what a printed text will look like at this place. If you read this text, you will get no information. Really? Is there no information? Is there a difference between this text and some nonsense like "Huardest gefburn"? Kjift – not at all! A blind text like this gives you information about the selected font, how the letters are written and an impression of the look. This text should contain all letters of the alphabet and it should be written in of the original language. There is no need for special content, but the length of words should match the language.

1.2.3 Simulation methods

Hello, here is some text without a meaning. This text should show what a printed text will look like at this place. If you read this text, you will get no information.

Really? Is there no information? Is there a difference between this text and some nonsense like “Huardest gefburn”? Kjift – not at all! A blind text like this gives you information about the selected font, how the letters are written and an impression of the look. This text should contain all letters of the alphabet and it should be written in of the original language. There is no need for special content, but the length of words should match the language.

Numerical solution of nonlinear ODEs

Hello, here is some text without a meaning. This text should show what a printed text will look like at this place. If you read this text, you will get no information. Really? Is there no information? Is there a difference between this text and some nonsense like “Huardest gefburn”? Kjift – not at all! A blind text like this gives you information about the selected font, how the letters are written and an impression of the look. This text should contain all letters of the alphabet and it should be written in of the original language. There is no need for special content, but the length of words should match the language.

Boundary value problem for limit cycle models

Hello, here is some text without a meaning. This text should show what a printed text will look like at this place. If you read this text, you will get no information. Really? Is there no information? Is there a difference between this text and some nonsense like “Huardest gefburn”? Kjift – not at all! A blind text like this gives you information about the selected font, how the letters are written and an impression of the look. This text should contain all letters of the alphabet and it should be written in of the original language. There is no need for special content, but the length of words should match the language.

1.2.4 ODE Sensitivity Analysis

Hello, here is some text without a meaning. This text should show what a printed text will look like at this place. If you read this text, you will get no information. Really? Is there no information? Is there a difference between this text and some nonsense like “Huardest gefburn”? Kjift – not at all! A blind text like this gives you information about the selected font, how the letters are written and an impression of the look. This text should contain all letters of the alphabet and it should be written in of the original language. There is no need for special content, but the length of words should match the language.

ODEs in general

Hello, here is some text without a meaning. This text should show what a printed text will look like at this place. If you read this text, you will get no information. Really? Is there no information? Is there a difference between this text and some nonsense like “Huardest gefburn”? Kjift – not at all! A blind text like this gives you information about the selected font, how the letters are written and an impression of the look. This text should contain all letters of the alphabet and it should be written in of the original language. There is no need for special content, but the length of words should match the language.

Period sensitivity

Hello, here is some text without a meaning. This text should show what a printed text will look like at this place. If you read this text, you will get no information. Really? Is there no information? Is there a difference between this text and some nonsense like “Huardest gefburn”? Kjift – not at all! A blind text like this gives you information about the selected font, how the letters are written and an impression of the look. This text should contain all letters of the alphabet and it should be written

in of the original language. There is no need for special content, but the length of words should match the language.

PRCs

Hello, here is some text without a meaning. This text should show what a printed text will look like at this place. If you read this text, you will get no information. Really? Is there no information? Is there a difference between this text and some nonsense like “Huardest gefburn”? Kjift – not at all! A blind text like this gives you information about the selected font, how the letters are written and an impression of the look. This text should contain all letters of the alphabet and it should be written in of the original language. There is no need for special content, but the length of words should match the language.

1.2.5 Previous models of circadian rhythms

Hello, here is some text without a meaning. This text should show what a printed text will look like at this place. If you read this text, you will get no information. Really? Is there no information? Is there a difference between this text and some nonsense like “Huardest gefburn”? Kjift – not at all! A blind text like this gives you information about the selected font, how the letters are written and an impression of the look. This text should contain all letters of the alphabet and it should be written in of the original language. There is no need for special content, but the length of words should match the language.

Chapter 2

A new model of the core circadian feedback loop

2.1 Biological Motivation

The functional roles of the cryptochrome isoforms (*Cry1* and *Cry2*) in circadian rhythms have long eluded biologists, as although they share a similar structure, perturbations to these genes typically result in opposite trends [2]. Existing genetic evidence and siRNA knockdown studies agree that while suppressing *Cry1* leads to shorter periods, suppressing *Cry2* leads to longer periods [3, 4]. However, some evidence shows the similarity between the two *Crys*. The knockouts $Cry1^{+/-}$ $Cry2^{-/-}$ and $Cry1^{-/-}$ $Cry2^{+/-}$ both show shorter wheel-running activity their respective WT/double knockouts $Cry1^{+/+}$ $Cry2^{-/-}$ and $Cry1^{-/-}$ $Cry2^{+/+}$ [3].

In unpublished work, experimental collaborators from Steve Kay's lab in UCSD have identified a small molecule modulator of cryptochrome through forward chemical genetic screening. The compound was found to simultaneously increase the half-life of CRY and cause period lengthening. The molecule, a carbazole derivative, is tentatively named KL001. In order to explain these new experimental results while

maintaining consistency with published evidence, I constructed a simple mathematical model of the Per/Cry negative feedback loop. The design of the model was inspired by the experimental evidence described below:

2.1.1 Network Structure

In the core feedback loop, Per and Cry transcription is activated by the CLOCK-BMAL1 complex. The protein products of these genes are transported to the nucleus after a time delay and bind to CLOCK-BMAL1, repressing their own transcription. Evidence indicates that an interaction of PER and CRY proteins is required for the timely nuclear entry of both proteins [5, 6, 7]. I therefore assume that PER and CRY bind and enter the nucleus in a 1:1 stoichiometric ratio, similar to more complicated models of mammalian circadian rhythms [8, 9, 10].

2.1.2 Protein Stoichiometry

Quantitative protein assays have revealed that the PER proteins are present at levels nearly ten times less than the CRYs, and are completely consumed at their trough. The CRYs, on the other hand, only fall to about one quarter of their peak value [11]. These results indicate that PER is the rate-limiting component for nuclear entry. This configuration explains why, since /it Cry is in excess, a knockout of either *Cry* does not lead to loss of function at the tissue level. Additionally *Cry1*, the more dominant repressor, is consistently found at higher levels than *Cry2*. However, since the ratio of nuclear to total protein is nearly equivalent for CRY1 and CRY2, PER must import each with equal affinity [11, 12].

2.1.3 Importance of Degradation

Studies of the simplest cellular oscillators have illustrated the importance of the degradation of repressor complexes in determining the period of oscillation [13]. In the mammalian circadian clock, FBXL3 has been indicated as a key protein in clearing the nucleus of CRY, and siRNA knockdowns of *Fbxl3* result in period lengthening [4]. While FBXL3 localizes primarily in the nucleus, CRY2 possesses a distinct phosphorylation domain that flags it for cytosolic proteolysis [14]. Knocking down this domain shortens the period, indicating that degradation rates play a major role in determining the oscillatory period and that stabilization in the cytosol and nucleus are likely not equivalent.

2.1.4 Key Time Delays

Similar to *Drosophila*, mammalian circadian oscillations are generated by three main time delays in the negative feedback loop: mRNA transcription, nuclear localization of protein, and degradation of the nuclear complexes [15]. In order to capture these dynamics without introducing unnecessary stiffness, I explicitly consider only the concentrations of nuclear mRNA, cytosolic unbound protein, and nuclear protein complexes.

2.2 A New Model for Period Regulation

Since the circadian clock is largely insensitive to the total amount *Cry*, it follows that the core negative loop is comprised of two redundant coupled inhibitory mechanisms. The natural periods of these two loops (running in isolation of the other) can be inferred from their corresponding knockout phenotype, i.e., the CRY1 feedback loop has a long period, while the CRY2 loop has a short period. In the wild-type phenotype, the two isoforms of CRY must compete for the available PER, and thus

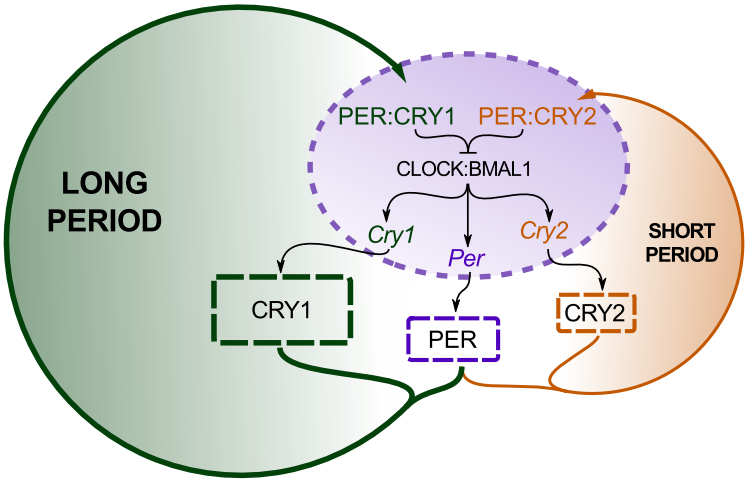

Figure 2.1: Model Connectivity. Schematic for the core negative feedback loop, consisting of the two redundant *Cry* mechanisms. The wild-type period, consisting of both loops, is a balance between the short and long oscillations.

the nuclear CRY1/CRY2 levels are constrained with a ratio proportional to their relative expression. This suggests that the period of the clock is governed by the nuclear CRY1/CRY2 ratio, where higher amounts of *Cry1* shift the clock closer to the $Cry2^{-/-}$ phenotype, and higher amounts of *Cry2* shift the clock closer to the $Cry1^{-/-}$ phenotype, described in figure 2.1.

2.3 The CRY1/CRY2 Ratio

In silico modeling was used to test the feasibility of the above hypothesis, and to investigate possible mechanisms by which the CRY1/CRY2 ratio might control the period of oscillations. The model uses eight state variables for the three mRNA species (*Per*, *Cry1*, and *Cry2*), three cytosolic proteins, and two nuclear proteins. The differential equations for each state were formulated using standard Hill-type repression, Michaelis-Menten, and mass action kinetics. The 21 unknown kinetic parameters were found by fitting the stoichiometric data from [11], requiring correct periods for

the $Cry1^{-/-}$ and $Cry2^{-/-}$ knockouts.

I investigated two possible mechanisms to explain the long/short period phenotype of the CRY1/CRY2 loops. First, following experimental evidence, I allowed CRY1 and CRY2 to have different inhibitory efficiency [16]. However, optimizations with this structure were unable to find a parameter set with appropriate period sensitivities, described in section 2.7. Instead, I investigated whether the difference in potency between *Crys* could be explained through difference in degradation rates. To this end, I allowed the degradation rates of nuclear CRY1 and CRY2 to differ, while holding their inhibition constants equal. Using this configuration, the structure was able to fit the experimental sensitivities. In the optimized parameter set, the degradation rate of nuclear CRY2 is higher than that of CRY1, such that for a constant total nuclear CRY, higher fractions of CRY2 cause the repressive complexes to be cleared faster. Since PER is the limiting reagent in nuclear entry, the amount of total CRY that enters the nucleus is largely insensitive to perturbations in cytosolic CRY expression. In effect, the two isoforms of CRY must compete for the available PER, and thus the nuclear CRY1/CRY2 levels are constrained with a ratio proportional to their relative expression. The period of the clock is thus governed by the nuclear CRY1/CRY2 ratio, where higher amounts of *Cry1* shift the clock closer to the $Cry2^{-/-}$ phenotype, and higher amounts of *Cry2* shift the clock closer to the $Cry1^{-/-}$ phenotype. Figure 2.2 shows the time varying total complex concentration under various perturbations, with the relative contributions from CRY1 and CRY2 highlighted.

2.4 Model Equations

The model is formulated as set of 8 ordinary differential equations shown in tables 2.1 and 2.2. Additional assumptions made while formulating the model equations

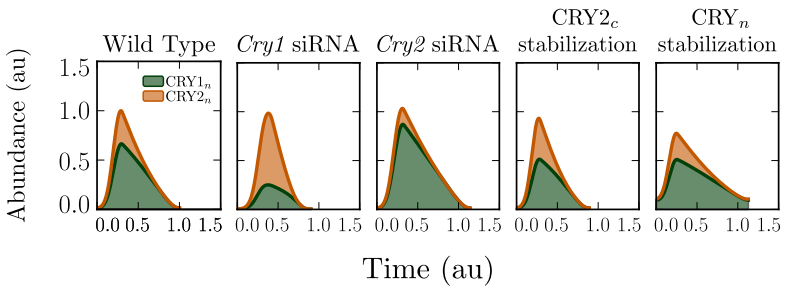

Figure 2.2: Degradation Profiles. Time course plots of the simulated total nuclear repressor concentration for the degradation model under various clock conditions. The relative contribution of CRY1 and CRY2 are shaded green and orange, respectively. Longer periods occur when a higher percentage of the nuclear complex is CRY1, taking longer to degrade.

are listed below:

- For simplicity and ease of parameter estimation, the model only considers the three genes *Per*, *Cry1*, and *Cry2*, not explicitly considering the three known isoforms of *Per*.

- EBOX activators *Clock* and *Bmal1* are considered constitutively expressed and are represented by the v_{txn} parameters.

- Repression of CLOCK-BMAL1 activity is attained through Hill-type inhibition. The Hill coefficient is fixed at 3, which was found to provide sufficient nonlinearity for oscillations. See below for the derivation of the repressor input function used in tables S2A and S2B.

- The degradation of the mRNA species and cytoplasmic proteins is assumed to follow standard Michaelis-Menten kinetics.

- The degradation kinetics of the nuclear proteins are assumed to follow Michaelis-Menten kinetics. Because both CRY1_n and CRY2_n are thought to be degraded by the same pathway in the nucleus, kinetic equations using the *pseudo* steady-

state hypothesis were derived for two substrates sharing the same enzyme. As a result, each *Cry* isoform acts as an inhibitor to the other's degradation.

Table 2.1: Model Equations for the Degradation Model. Lower case letters (p: *Per*, c1: *Cry1*, c2: *Cry2*) are mRNA state variables. Uppercase letters (P: PER, C1: CRY1, C2: CRY2) are the free (cytosolic) proteins. C1N: CRY1 and C2N: CRY2 are the nuclear proteins.

$$\frac{d\mathbf{p}}{dt} = \frac{v_{\text{txn},\mathbf{p}}}{k_{\text{txn},\mathbf{p}} + (\mathbf{C1N} + \mathbf{C2N})^3} - \frac{v_{\text{deg},\mathbf{p}}\ \mathbf{p}}{k_{\text{deg},\mathbf{p}} + \mathbf{p}} \tag{2.1}$$

$$\frac{d\mathbf{c1}}{dt} = \frac{v_{\text{txn},\mathbf{c1}}}{k_{\text{txn},\mathbf{c}} + (\mathbf{C1N} + \mathbf{C2N})^3} - \frac{v_{\text{deg},\mathbf{c1}}\ \mathbf{c1}}{k_{\text{deg},\mathbf{c}} + \mathbf{c1}} \tag{2.2}$$

$$\frac{d\mathbf{c2}}{dt} = \frac{v_{\text{txn},\mathbf{c2}}}{k_{\text{txn},\mathbf{c}} + (\mathbf{C1N} + \mathbf{C2N})^3} - \frac{v_{\text{deg},\mathbf{c2}}\ \mathbf{c2}}{k_{\text{deg},\mathbf{c}} + \mathbf{c2}} \tag{2.3}$$

$$\begin{aligned}\frac{d\mathbf{P}}{dt} = {} & k_{\text{tln},\mathbf{p}}\ \mathbf{p} - \frac{v_{\text{deg},\mathbf{P}}\ \mathbf{P}}{k_{\text{deg},\mathbf{P}} + \mathbf{P}} - v_{\text{a},\mathbf{CP}}\ \mathbf{P}\ \mathbf{C1} + v_{\text{d},\mathbf{CP}}\ \mathbf{C1N} \\ & - v_{\text{a},\mathbf{CP}}\ \mathbf{P}\ \mathbf{C2} + v_{\text{d},\mathbf{CP}}\ \mathbf{C2N}\end{aligned} \tag{2.4}$$

$$\frac{d\mathbf{C1}}{dt} = \mathbf{c1} - \frac{v_{\text{deg},\mathbf{C1}}\ \mathbf{C1}}{k_{\text{deg},\mathbf{C}} + \mathbf{C1}} - v_{\text{a},\mathbf{CP}}\ \mathbf{P}\ \mathbf{C1} + v_{\text{d},\mathbf{CP}}\ \mathbf{C1N} \tag{2.5}$$

$$\frac{d\mathbf{C2}}{dt} = \mathbf{c2} - \frac{v_{\text{deg},\mathbf{C2}}\ \mathbf{C2}}{k_{\text{deg},\mathbf{C}} + \mathbf{C2}} - v_{\text{a},\mathbf{CP}}\ \mathbf{P}\ \mathbf{C2} + v_{\text{d},\mathbf{CP}}\ \mathbf{C2N} \tag{2.6}$$

$$\frac{d\mathbf{C1N}}{dt} = -\frac{v_{\text{deg},\mathbf{CP}}\ \mathbf{C1N}}{k_{\text{deg},\mathbf{CP}} + \mathbf{C1N} + \mathbf{C2N}} + v_{\text{a},\mathbf{CP}}\ \mathbf{P}\ \mathbf{C1} - v_{\text{d},\mathbf{CP}}\ \mathbf{C1N} \tag{2.7}$$

$$\frac{d\mathbf{C2N}}{dt} = -\frac{\left(v_{\text{deg},\mathbf{CP}}\ m_{\mathbf{C2N}}\right)\ \mathbf{C2N}}{k_{\text{deg},\mathbf{CP}} + \mathbf{C2N} + \mathbf{C1N}} + v_{\text{a},\mathbf{CP}}\ \mathbf{P}\ \mathbf{C2} - v_{\text{d},\mathbf{CP}}\ \mathbf{C2N} \tag{2.8}$$

2.5 Derivation of a Shared Enzyme Degradation Rate

To find the rate equations associated with a shared-enzyme degradation mechanism, we derive them from the equilibrium relationships:

$$[\text{E}] + [\text{S1}] \underset{k_{-1}}{\overset{k_1}{\rightleftharpoons}} [\text{ES1}] \xrightarrow{k_{d,1}} [\text{E}]$$

Table 2.2: Changed Equations for the Activation-based Model. The remainder of the model equations (not duplicated below) are found in table 2.1

$$\frac{d\mathbf{p}}{dt} = \frac{v_{\text{txn},\mathbf{p}}}{k_{\text{txn},\mathbf{p}} + (m_{\mathbf{C2N}}\,\mathbf{C1N} + \mathbf{C2N})^3} - \frac{v_{\text{deg},\mathbf{p}}\;\mathbf{p}}{k_{\text{deg},\mathbf{p}} + \mathbf{p}} \tag{2.1*}$$

$$\frac{d\mathbf{c1}}{dt} = \frac{v_{\text{txn},\mathbf{c1}}}{k_{\text{txn},\mathbf{c}} + (m_{\mathbf{C2N}}\,\mathbf{C1N} + \mathbf{C2N})^3} - \frac{v_{\text{deg},\mathbf{c1}}\;\mathbf{c1}}{k_{\text{deg},\mathbf{c}} + \mathbf{c1}} \tag{2.2*}$$

$$\frac{d\mathbf{c2}}{dt} = \frac{v_{\text{txn},\mathbf{c2}}}{k_{\text{txn},\mathbf{c}} + (m_{\mathbf{C2N}}\,\mathbf{C1N} + \mathbf{C2N})^3} - \frac{v_{\text{deg},\mathbf{c2}}\;\mathbf{c2}}{k_{\text{deg},\mathbf{c}} + \mathbf{c2}} \tag{2.3*}$$

$$\frac{d\mathbf{C2N}}{dt} = -\frac{v_{\text{deg},\mathbf{CP}}\;\mathbf{C2N}}{k_{\text{deg},\mathbf{CP}} + \mathbf{C2N} + \mathbf{C1N}} + v_{\text{a},\mathbf{CP}}\;\mathbf{P}\;\mathbf{C2} - v_{\text{d},\mathbf{CP}}\;\mathbf{C2N} \tag{2.8*}$$

$$[\text{E}] + [\text{S2}] \underset{k_{-2}}{\overset{k_2}{\rightleftharpoons}} [\text{ES2}] \xrightarrow{k_{d,2}} [\text{E}]$$

$$[\text{E}_t] = [\text{E}] + [\text{ES1}] + [\text{ES2}] \tag{2.9}$$

The end goal is the degradation rates of the two enzyme complexes:

$$\begin{aligned} r_{d,1} &= k_{d,1}\,[\text{ES1}] \\ r_{d,2} &= k_{d,2}\,[\text{ES2}] \end{aligned} \tag{2.10}$$

We invoke the standard pseudo steady-state assumption and set $\frac{d[\text{ES}]}{dt} = 0$, and obtain the following production = consumption equalities for [ES1]:

$$k_1[\text{E}][\text{S}] = k_{-1}[\text{ES1}] + k_{d,1}[\text{ES1}] \tag{2.11}$$

Solving eq. 2.11 for ES1 and substituting in eq. 2.9, we obtain

$$\left(\frac{k_{-1} + k_{d,1}}{k_1}\right)[\text{ES1}] = ([\text{E}_t] - [\text{ES1}] - [\text{ES2}])\,[\text{S1}]$$

Table 2.3: Parameter Set. Parameters for model described in table 2.1.

	Parameter	Description	Degradation	Activation
1	$v_{\text{txn},\mathbf{p}}$	*Per* Transcription rate	0.195	0.276
2	$v_{\text{txn},\mathbf{c1}}$	*Cry1* Transcription rate	0.131	0.062
3	$v_{\text{txn},\mathbf{c2}}$	*Cry1* Transcription rate	0.114	0.053
4	$k_{\text{txn},\mathbf{p}}$	*Per* Repression constant	0.425	0.425
5	$k_{\text{txn},\mathbf{c}}$	*Cry1/2* Repression constant	0.259	0.262
6	$v_{\text{deg},\mathbf{p}}$	*Per* Max degradation rate	0.326	0.472
7	$v_{\text{deg},\mathbf{c1}}$	*Cry1* Max degradation rate	0.676	0.322
8	$v_{\text{deg},\mathbf{c2}}$	*Cry2* Max degradation rate	0.608	0.290
9	$k_{\text{deg},\mathbf{p}}$	*Per* Degradation constant	0.011	0.024
10	$k_{\text{deg},\mathbf{c}}$	*Cry1/2* Degradation constant	1.149	0.809
11	$v_{\text{deg},\mathbf{P}}$	Max PERc degradation rate	2.970	2.970
12	$k_{\text{deg},\mathbf{P}}$	PERc degradation constant	0.034	0.034
13	$v_{\text{deg},\mathbf{C1}}$	Max CRY1c degradation rate	1.523	1.048
14	$v_{\text{deg},\mathbf{C2}}$	Max CRY2c degradation rate	1.686	1.134
15	$k_{\text{deg},\mathbf{C}}$	CRYc degradation constant	2.017	2.028
16	$v_{\text{deg},\mathbf{CP}}$	CRYn degradation rate	0.101	0.070
17	$m_{\mathbf{C2N}}$	CRY2n degradation multiplier	3.318	3.334
18	$k_{\text{deg},\mathbf{CP}}$	CRYn degradation constant	0.053	0.053
19	$v_{\text{a},\mathbf{CP}}$	CRYn association rate	0.041	0.028
20	$v_{\text{d},\mathbf{CP}}$	CRYn dissociation rate	0.002	0.001
21	$k_{\text{tln},\mathbf{p}}$	PER translation rate	3.000	1.000

After defining a useful combined rate constant,

$$K_1 \equiv \frac{k_{-1} + k_{d,1}}{k_1}$$

we can further simplify

$$\begin{aligned} K_1[\text{ES1}] + [\text{S1}][\text{ES1}] &= ([\text{E}_t] - [\text{ES2}])[\text{S1}] \\ [\text{ES1}] &= \frac{([\text{E}_t] - [\text{ES2}])[\text{S1}]}{K_1 + [\text{S1}]} \end{aligned} \tag{2.12}$$

If we perform the same operations for [ES2] and plug them into equation 2.12.

$$
\begin{aligned}
[\mathrm{ES1}] &= \frac{\left(\mathrm{E}_t] - \frac{([\mathrm{E}_t]-[\mathrm{ES1}])[\mathrm{S2}]}{K_2+[\mathrm{S2}]}\right)\mathrm{S1}]}{K_1+[\mathrm{S1}]} \\
[\mathrm{ES1}] &= \frac{[\mathrm{E}]_t[\mathrm{S1}]}{K_1+[\mathrm{S1}]} - \frac{[\mathrm{E}]_t[\mathrm{S1}][\mathrm{S2}]}{(K_1+[\mathrm{S1}])(K_2+[\mathrm{S2}])} + \frac{[\mathrm{ES1}][\mathrm{S1}][\mathrm{S2}]}{(K_1+[\mathrm{S1}])(K_2+[\mathrm{S2}])} \\
[\mathrm{ES1}] &= \left(\frac{[\mathrm{E}]_t[\mathrm{S1}]}{K_1+[\mathrm{S1}]}\right)\left(\frac{1-\frac{[\mathrm{S2}]}{K_2+[\mathrm{S2}]}}{1-\frac{[\mathrm{S1}][\mathrm{S2}]}{(K_1+[\mathrm{S1}])(K_2+[\mathrm{S2}])}}\right)
\end{aligned}
\tag{2.13}
$$

If we pull the second fraction from (2.13) into the denominator of the first, we can simplify further.

$$
\begin{aligned}
[\mathrm{ES1}] &= \frac{[\mathrm{E}]_t[\mathrm{S1}]}{\left(\frac{K_1+[\mathrm{S1}]-\frac{[\mathrm{S1}][\mathrm{S2}]}{K_2+[\mathrm{S2}]}}{1-\frac{[\mathrm{S2}]}{K_2+[\mathrm{S2}]}}\right)} \\
[\mathrm{ES1}] &= \frac{[\mathrm{E}]_t[\mathrm{S1}]}{\left(\frac{K_2+[\mathrm{S2}]}{K_2}\right)\left(K_1+[\mathrm{S1}]-\frac{[\mathrm{S1}][\mathrm{S2}]}{K_2+[\mathrm{S2}]}\right)} \\
[\mathrm{ES1}] &= \frac{K_2[\mathrm{E}]_t[\mathrm{S1}]}{(K_1+[\mathrm{S1}])(K_2+[\mathrm{S2}])-[\mathrm{S1}][\mathrm{S2}]} \\
[\mathrm{ES1}] &= \frac{K_2[\mathrm{E}]_t[\mathrm{S1}]}{K_1K_2+K_2[\mathrm{S1}]+K_1[\mathrm{S2}]} \\
[\mathrm{ES1}] &= \frac{K_2[\mathrm{E}]_t[\mathrm{S1}]}{K_1K_2+K_2[\mathrm{S1}]+K_1[\mathrm{S2}]}
\end{aligned}
$$

Dividing top and bottom by K2:

$$
[\mathrm{ES1}] = \frac{[\mathrm{E}]_t[\mathrm{S1}]}{K_1+[\mathrm{S1}]+\frac{K_1}{K_2}[\mathrm{S2}]} \tag{2.14}
$$

Substituting (2.14) into (2.10) and setting $K_1 = K_2$, $k_{d,1} \neq k_{d,2}$, we obtain the final shared rate laws (with an equivalent analysis for [ES2])

$$r_{d,1} = \frac{V_{\max,1}[\text{S1}]}{K_M + [\text{S1}] + [\text{S2}]}$$

$$r_{d,2} = \frac{V_{\max,2}[\text{S2}]}{K_M + [\text{S1}] + [\text{S2}]}$$

2.6 Derivation of Hill-type Repression Formulas

To derive the equations for the Hill-type inhibition, allowing for different repressive activities (table 2.2), we start with the standard equation for Hill-type regulation:

$$\frac{v_{\max}[A]^n}{K_m^n + [A]^n} \tag{2.15}$$

Allowing for competitive inhibition with two inhibitors, K_m is replaced with the apparent Michaelis-Menten constant

$$K_m^{\text{app}} = K_m \left(1 + \frac{[I_1]}{K_{i,1}} + \frac{[I_2]}{K_{i,2}}\right) \tag{2.16}$$

By assuming constitutive activator concentrations and non-dimensionalizing $[I^\star] = \frac{[I]}{K_{i,2}}$, $m = \frac{K_{i,2}}{K_{i,1}}$:

$$\frac{v_{\max^\star}}{K_m^\star + \left(m\,[I_1^\star] + [I_2^\star]\right)^n}$$

Assuming equal repressive activity ($K_{i,2} = K_{i,1}$), $m = 1$, we obtain the rate equation used in the degradation model.

2.7 Parameter Estimation

The model equations, specifying the state and parameter dependent time derivatives of each concentration variable, were written in python using the CasADi computer algebra package [17]. The model was simulated using the SUNDIALS suite of ODE solvers [18]. A parameter-dependent cost function was developed that assigns numerical values reflecting how well a parameter set fits desired features, taken from [11]. The first step in the cost function evaluation is the numerical solution of the limit cycle, described previously [19]. If a limit cycle was unable to be found, the cost function returns a maximum value. Otherwise, the cost function returns a squared difference from the desired value. A priority weight was also attached to each cost entry, such that more important costs would be prioritized. A description of each entry in the cost function, along with the value for experimental and final model is shown in table 2.4 (degradation-based model, table 2.1; activation-based model, table 2.2). To minimize the cost function, we employed a genetic algorithm method used previously for optimizing circadian parameters [9]. In the method, 5000 solutions are calculated at random parameter values within feasible bounds. Those with the best cost function scores are kept and used to generate subsequent solutions. This procedure is iterated for up to 2000 generations, or until convergence criteria are met.

Table 2.4: Summary of Cost Function Entries. The weights for each entry were chosen based on the relative importance of the desired behavior. Entries 1-9 and 12-16 were obtained from the data presented in [11]. SiRNA sensitivities were obtained were taken from [4].

	Description	Weight	Desired	Degradation	Activation
1	*per* mRNA peak-trough ratio $\frac{y_{\max}(Per)}{y_{\min}(Per)}$	0.5	> 20	large	large
2	*Cry1* mRNA peak-trough ratio $\frac{y_{\max}(Cry1)}{y_{\min}(Cry1)}$	0.5	2.155	8.942	3.748
3	*Cry2* mRNA peak-trough ratio $\frac{y_{\max}(Cry2)}{y_{\min}(Cry2)}$	0.5	2.236	7.813	3.484
4	PER protein peak to trough ratio $\frac{y_{\max}(\mathrm{PER})}{y_{\min}(\mathrm{PER})}$	5	> 20	large	large

	Description	Weight	Desired	Degradation	Activation
5	CRY1 protein peak-trough ratio $\frac{y_{\max}(\text{CRY1})}{y_{\min}(\text{CRY1})}$	3	3.247	6.385	1.847
6	CRY2 protein peak-trough ratio $\frac{y_{\max}(\text{CRY2})}{y_{\min}(\text{CRY2})}$	3	1.975	8.094	2.347
7	Fraction PER of total protein $\frac{y_{\max}(\text{PER})}{y_{\max}(\text{PER}) + y_{\max}(\text{CRY1}) + y_{\max}(\text{CRY2})}$	3	0.105	0.169	0.073
8	Fraction CRY1 of total protein $\frac{y_{\max}(\text{CRY1})}{y_{\max}(\text{PER}) + y_{\max}(\text{CRY1}) + y_{\max}(\text{CRY2})}$	3	0.555	0.473	0.554
9	Fraction CRY2 of total protein $\frac{y_{\max}(\text{CRY2})}{y_{\max}(\text{PER}) + y_{\max}(\text{CRY1}) + y_{\max}(\text{CRY2})}$	3	0.341	0.358	0.373

	Description	Weight	Desired	Degradation	Activation
10	*Cry1* siRNA period sensitivity $\frac{\partial T}{\partial v_{\text{deg},\mathbf{c1}}}$	5	< 0	< 0	> 0
11	*Cry2* siRNA period sensitivity $\frac{\partial T}{\partial v_{\text{deg},\mathbf{c2}}}$	5	> 0	> 0	< 0
12	*Cry1* knockout period $\frac{T(Cry1^{-/-})}{T(\text{WT})}$	5	$< 95\%$	92.1%	193.4%
13	*Cry2* knockout period $\frac{T(Cry2^{-/-})}{T(\text{WT})}$	5	$> 115\%$	131.8%	99.4%
14	Fraction CRY1 entering nucleus $\frac{y_{\max}(\text{CRY1}_n)}{y_{\max}(\text{CRY1} + \text{CRY1}_n)}$	1	0.40	0.195	0.059

	Description	Weight	Desired	Degradation	Activation
15	Fraction CRY2 entering nucleus $\frac{y_{\max}(\text{CRY2}_n)}{y_{\max}(\text{CRY2} + \text{CRY2}_n)}$	1	0.35	0.139	0.059
16	Time delay between nuclear repressors and mRNA $t_{\max}(\text{nuclear protein}) - t_{\max}(\text{mRNA})$	3	75%	0.850	0.848
17	Time delay between mRNA and cytoplasmic protein $t_{\max}(\text{mRNA}) - t_{\max}(\text{protein})$	3	25%	0.057	0.095
18	Time delay between cytoplasmic protein and nuclear protein $t_{\max}(\text{protein}) - t_{\max}(\text{nuclear protein})$	3	0%	0.093	0.057

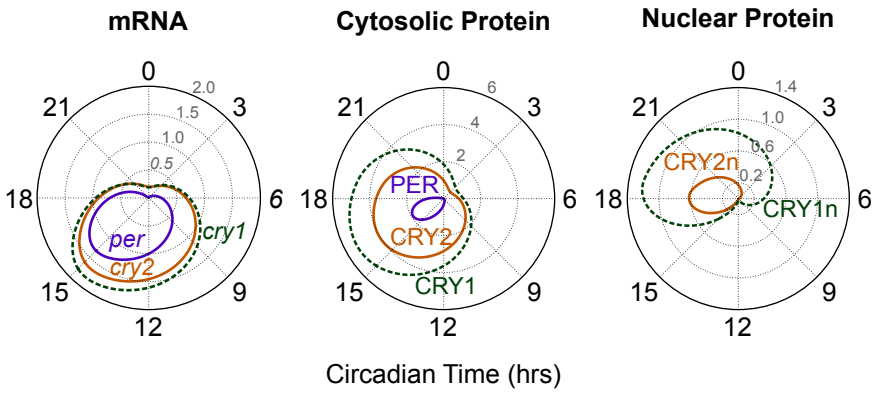

Figure 2.3: Time Course Plots. The three polar plots show the time-varying levels of each clock component for optimal parameter set. In these plots, the amplitude of each variable (always positive) is plotted against its phase, $0 \rightarrow 2\pi$. Since the limit cycle is periodic, this results in a closed curve. Rising mRNA levels caused by low repressor concentrations (CT12) result in accumulating cytosolic protein (left plot). Lower levels of PER prevent all the available CRY from entering the nucleus (middle plot). High levels of nuclear repressors halt transcription until both CRYs have degraded (right plot).

2.8 Model Validation and Dynamics

The model was validated by comparing the simulated dynamics to experimental measurements. First, the time course plots of the state variables display reasonable phases and amplitudes, and oscillate with a period of 23.7 hours (figure 2.3. The knockout periods are 21.7 hr (91.4% of WT) for $Cry1^{-/-}$ and 31.5 hr (133% of WT) for $Cry2^{-/-}$, indicating that the two feedback loops are indeed redundant with different free-running periods.

2.8.1 SiRNA knockdowns

SiRNA knockdowns were performed *in silico* by increasing the degradation rate for the corresponding mRNA; shown in figure 2.4, as done previously in [20]. *Cry1* and *Cry2* knockdowns in wild type conditions show close agreement to experiment [4], and demonstrate that altering the nuclear CRY1/CRY2 ratio is effective in changing

the period of oscillation.

2.8.2 CRY2 Cytosolic Stabilization

The *Dyrk1a* knockdown in [14] serves as another demonstration of the change in period as a response to a change in nuclear CRY1/CRY2 ratio. To demonstrate the effect in silico, the degradation rate of cytosolic CRY2 was decreased. Matching experimental evidence, the cytosolic CRY2 levels rose, with a corresponding change in the nuclear CRY ratio and decrease in period.

2.8.3 Single Cry Perturbations

The $Cry1^{+/-}$ $Cry2^{-/-}$ and $Cry1^{-/-}$ $Cry2^{+/-}$ single/double knockout perturbations ([3]) were approximated with an appropriate knockout and siRNA knockdown, and show the correct period shortening. With one *Cry* knocked out, the levels of cytoplasmic PER are no longer stoichiometrically limiting. In this case, less *Cry* leads to less nuclear complex, which is cleared faster.

2.9 Prediction of KL001 Mechanism

Using the completed model, I investigated possible mechanisms by which KL001 might lengthen the circadian period. Experimental evidence indicates that stabilization of CRY can either lengthen the period (*Fbxl3* knockdown) or shorten the period (*Dyrk1a* knockdown). Assuming equal effect on both isoforms of *Cry*, the model confirms that cytoplasmic stabilization results in period shortening, since excess CRY expedites the nuclear import of the PER:CRY repressive complex. However, stabilizing nuclear CRY (figure 2.2, last column) yields the appropriate period lengthening observed experimentally. We therefore predicted that KL001 acts primarily in the nucleus, potentially through the FBXL3 degradation pathway. Additionally, the model

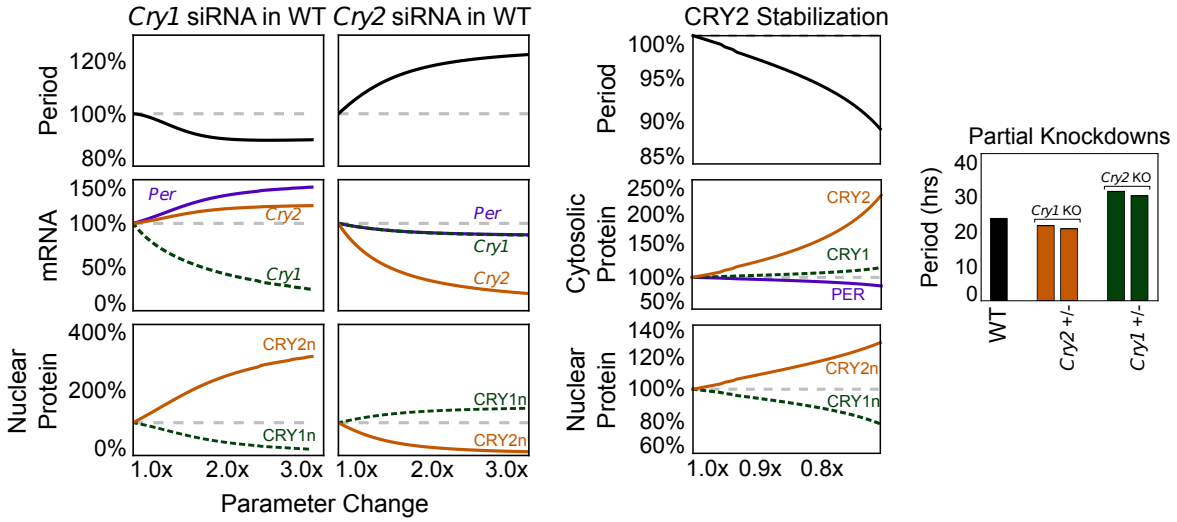

Figure 2.4: Model Validation. When comparing against existing experimental results, the model shows the correct response for *Cry1* siRNA, *Cry2* siRNA, and CRY_c stabilization (left, middle), through an adjustment in the nuclear CRY1/CRY2 ratio. The model also correctly captures the single/double knockout phenotype of [3], (right)

predicts that the compound's effect on $Cry1^{-/-}$ and $Cry2^{-/-}$ systems would be similar to its effect on the wild type clock, causing dose-dependent period lengthening (figure 2.5, left and right).

2.10 Experimental Confirmation

Experimental tests of the model's predictions were performed. Nuclear CRY1 and CRY2 levels were up-regulated and almost sustained, respectively, while PER1 level was strongly down-regulated by the compound, supporting stabilization of nuclear CRY, the predicted mechanism. Additionally, continuous treatment with KL001 lengthened the period in both *Cry1* and *Cry2* knockout cells in a dose-dependent manner. Similarly, the compound caused period lengthening in both CRY1 and CRY2 knockdown U2OS cells. We further investigated the effect of KL001 in SCN explants, which show robust rhythms even in the absence of *Cry1*, due to intercellular coupling

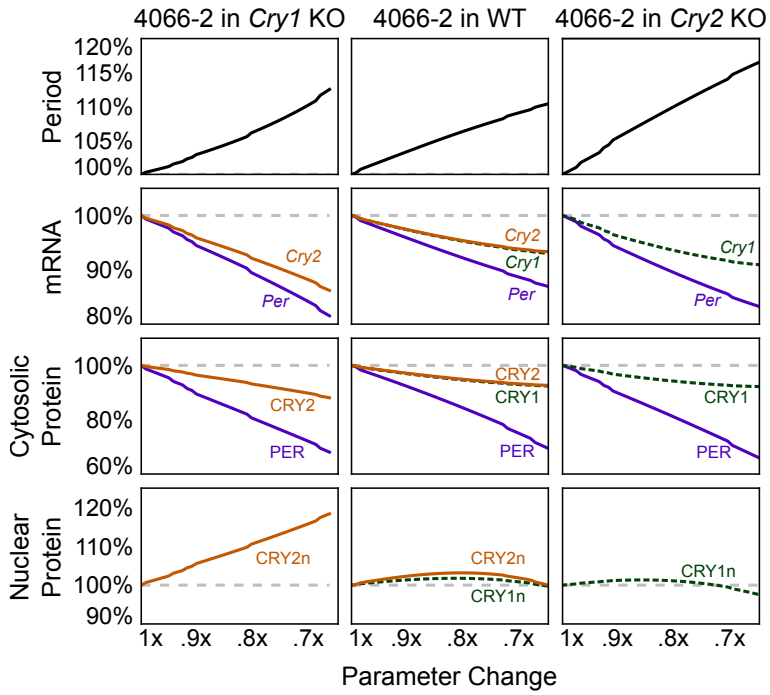

Figure 2.5: Model Prediction of the KL001 Mechanism. *In silico* response to equal stabilization of both CRYs in the nucleus results in longer periods (middle column), matching observed results. The model correctly predicts that stabilization of individual CRYs in the knockout environments also causes period lengthening.

[21]. Both *Cry1* and *Cry2* knockout SCN exhibited dose-dependent period lengthening by the compound treatment. Thus, in a single *Cry* knockout, stabilization of either nuclear CRY1 and CRY2 causes period lengthening, confirming model predictions.

2.11 Insights into Circadian Network Design

Mathematical modeling has revealed how the balancing of two redundant feedback loops can provide fine control over the oscillatory period. A contour plot of period vs CRY1 or CRY2 abundance is shown in figure 2.6, which shows that the model's period is largely insensitive to the total amount of CRY (45° line), but highly dependent on the ratio of the two isoforms. Sensitivity analysis of our mathematical model (figure 2.7) reveals that subtle changes in most of the involved rates can have

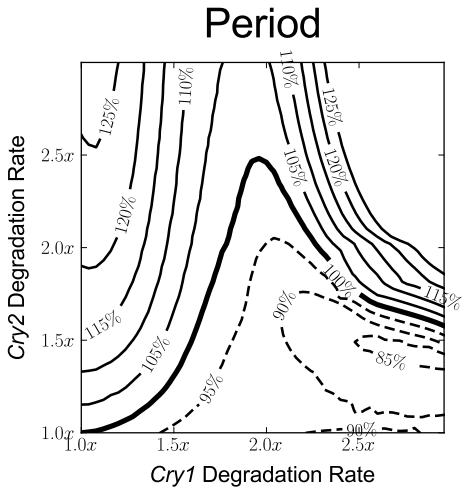

Figure 2.6: Simultaneous Knockdown of *Cry1* and *Cry2*. Period contours (% change) resulting from simultaneous *in silico* siRNA knockdowns of *Cry1* (x-axis) and *Cry2* (y-axis). The plot shows that the CRY1/CRY2 ratio determines the period, independent of total CRY, for perturbations up to twice the normal mRNA degradation rate.

an effect on the clock's free running period, which could be caused by evolutionary noise. Since many studies have linked entrainment to non-natural periods with long-term health problems, a mechanism to align the clock's natural period to that of the environment would be advantageous. It is therefore possible that the period control afforded by CRY1/CRY2 balancing is a deliberately conserved design principle of the circadian clock, which confers period robustness against random mutations of clock components. Indeed, the presence of independent control of the cytosolic CRY2 levels suggests that the biological clock can control its period through simple post-translational modifications [14].

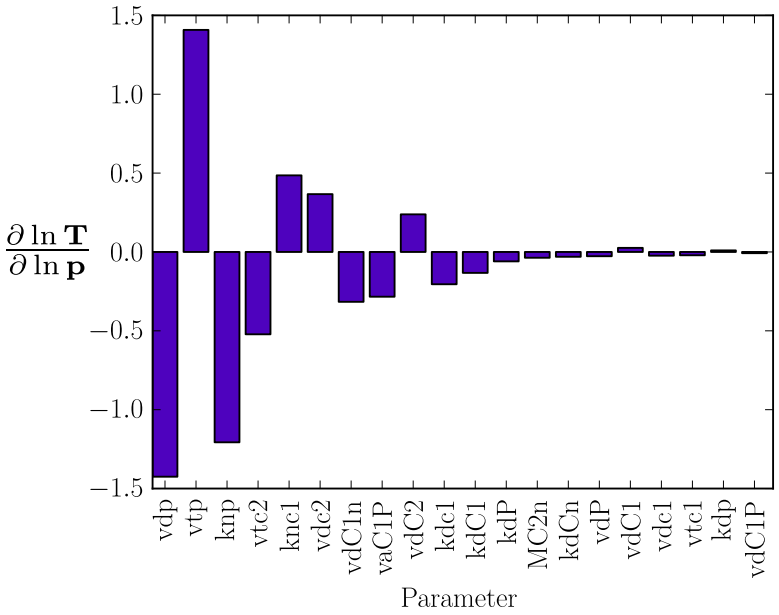

Figure 2.7: First Order Relative Period Sensitivities. Dimensionless period sensitivities with respect to the kinetic parameters in the degradation-based model. Perturbations to most clock rates result in noticeable changes to the free-running period. Many of the most sensitive parameters are transcriptional rates, which can be easily changed through mutation of DNA promoter regions.

Chapter 3

Identifiability analysis for models of circadian rhythms

3.1 Background

A cell's behavior is governed by the dynamic and selective expression of its genes, in which each protein's activity depends on a careful balance between transcription, translation, transport, and degradation rates. These rates, which change with environmental conditions and are often impossible to measure accurately *in vivo* or *in vitro*, determine the function of a regulatory pathway. While studying the roles of individual proteins can often provide some insight on how a particular function is achieved, this approach is limited in explaining complicated cellular phenomena at the scale of dozens to hundreds of interacting genes. With the aid of mathematical models, it is increasingly possible to create *in silico* realizations of genetic regulatory networks to examine their dynamic properties.

Essential to understanding how genetic circuits operate is connecting how inputs (i.e., environmental changes, extracellular signals) are processed to give the appropriate outputs (protein expression, cellular response). In some cases these quantities

may be changes to oscillatory profiles: for example, seasonal changes in day length leading to flowering or hibernation. Models of genetic regulatory networks, often sets of ordinary differential equations (ODEs), contain many unknown parameters that must be estimated from experimental data [22]. Derivatives of the model output with respect to changes in input, known as local sensitivities, are frequently validated experimentally or used to predict potential targets for pharmaceuticals [23]. Since sensitivities can change drastically with respect to the particular parameter values chosen, the confidence associated with parameter and sensitivity values is an important consideration in model analysis and design.

Practical identifiability analysis is concerned with calculating confidence intervals in parameter estimates resulting from uncertainty in experimental data [24]. Several techniques for such an analysis currently exist, and are commonly used in analyzing biological models [25, 26, 27]. In one method, the inverse of the Fisher information matrix is used to provide estimates of the variance in each parameter. However, since this method assumes a linearized model, the resulting symmetric normal distributions for each parameter do not accurately reflect the mapping of nonlinear models [28]. In the bootstrap method, distributions in parameter estimates are found through optimum fits to repeated physical or *in silico* measurements. While accurate in finding the true nonlinear confidence intervals, this approach requires efficient and robust parameter estimation convergence.

Many systems biology models focus on describing interesting dynamic features from interlocked regulatory mechanisms. Limit cycle oscillations are common features in many biological networks, ranging from cell cycle control to cyclic firing of cardiac cells and circadian rhythms [29]. In periodic systems, the behavior (and existence) of limit cycle oscillations is a discontinuous function of the parameters, complicating parameter estimation. Optimal values are traditionally found through trial-and-error type approaches [8, 10] or genetic algorithm search strategies [9], both

of which are not amenable to bootstrap methods. Additionally, since the solutions are oscillatory, additional care must be taken in the calculation of the first-order sensitivity values. Here we calculate the sensitivity of the oscillatory period to parameter perturbation, a biologically relevant quantity that is often measured experimentally [19]. Due to these complications, rigorous identifiability analyses of these models are typically not performed.

In this study, a bootstrap uncertainty analysis appropriate for oscillatory biological models is developed and applied to a previously published model of circadian rhythms [30]. Circadian rhythms are near 24-hour endogenous oscillations in physiological processes found in many organisms, coordinated through transcription-translation networks with inherent time-delayed negative feedback [6, 31, 32]. In mammals, expression of circadian E box genes Period (*Per*) and Cryptochrome (*Cry1* and *Cry2*) leads to elevated levels of their protein products, PER and CRY. The formation of a heterodimeric complex allows PER and CRY proteins enter the nucleus and subsequently suppress E box mediated transcription, resulting in rhythmic gene expression. These networks serve as an excellent example of a functional genetic circuit, able to process subtle environmental cues while remaining robust to temperature variations and evolutionary disturbances. Accurate limit cycle models must capture not only the correct time-dependent dynamics, but also the correct input-output response. For circadian rhythms, high-throughput microarrays have provided high-resolution time-series data of gene expression levels [33]. Additionally, knock-down experiments using RNA interference technology (siRNA) and small molecule modulators have resulted in a wealth of data on the dynamic responses to changes in key rates [4, 30, 34, 35]. This data, together with qualitative knowledge of the underlying network structure, permits the use and verification of a suitable uncertainty analysis.

To enable a bootstrap approach, we employ an efficient parameter estimation

routine optimized for limit cycle models. Motivated by the increasing availability of high-resolution time-series measurements, we use an approach similar to multiple shooting, in which a nonlinear and discontinuous parameter estimation problem is transformed into a high-dimensional yet local optimization and solved via nonlinear programming [36]. Since the desired shape of the limit cycle solution is known *a priori*, a relatively accurate initial guess for the parameters and trajectories can be found. By using multiple sets of *in silico* data of varying quality, we illustrate how error in experimental results is propagated to uncertainty in parameter sensitivity. Lower quality data - with either higher error or fewer sampling points - result in wider distributions of limit cycles and less identifiable responses. These results can be used in *a priori* experimental design, finding the minimum sampling points needed for an estimated experimental error to enable accurate modeling. Additionally, we show using literature data how this method can be used to discriminate between candidate model structures, revealing which one yields the highest predictive confidence.

3.2 Methods

3.2.1 Collocation Methods

In this work, the estimation of the unknown kinetic parameters is accomplished via nonlinear programming. The method is summarized here, taken primarily from [36]. In this method, we divide the limit cycle trajectory $\mathbf{x}(t, \mathbf{p})$ into $\mathcal{N}$ finite elements of length h, and approximate each with a $\mathcal{K}$ degree Lagrange interpolating polynomial,

$\mathbf{x}_i^{\mathcal{K}}(t)$, using an internal time $\tau \in [0,1]$. For finite element i:

$$\begin{aligned} t &= h(i+\tau) \\ \ell_j(\tau) &= \prod_{k=0,\neq j}^{\mathcal{K}} \frac{\tau - \tau_k}{\tau_j - \tau_k} \\ \mathbf{x}_i^{\mathcal{K}}(\tau) &= \sum_{j=0}^{\mathcal{K}} \ell_j(\tau)\ \mathbf{x}_{ij}. \end{aligned} \tag{3.1}$$

We also ensure that the interpolating polynomial matches system dynamics at each collocation point, τ_k, by setting

$$\begin{aligned} \sum_{j=0}^{\mathcal{K}} \mathbf{x}_{ij} \frac{d\ell_j(\tau_k)}{d\tau} &= h\mathbf{f}(\mathbf{x}_{ij}, \mathbf{p}) \\ \text{for} \quad k &= 1, \ldots, \mathcal{K}. \end{aligned} \tag{3.2}$$

Additionally, the interpolating polynomials for each finite element must form a continuous function, so the following continuity constraints are imposed:

$$\begin{aligned} \mathbf{x}_{i+1,0} &= \sum_{j=0}^{\mathcal{K}} \ell_j(1)\ \mathbf{x}_{i,j} \\ \text{for} \quad i &= 1, \ldots, \mathcal{N}-1. \end{aligned} \tag{3.3}$$

Periodic conditions are imposed by setting the beginning of the first element equal to the end of the final element:

$$\mathbf{x}_{0,0} = \sum_{j=0}^{\mathcal{K}} \ell_j(1)\ \mathbf{x}_{\mathcal{N},j} \tag{3.4}$$

The τ_k values are chosen for optimal accuracy, here we use Gauss-Radau roots so that the resulting method has stiff decay [36]. With $\mathcal{K} = 5$:

$$\tau = \{0.000, 0.057, 0.277, 0.584, 0.860, 1.000\}$$

The interpolating polynomials can now be compared to the experimental data. For each measured value, $\hat{\mathbf{x}}(t_n)$, the corresponding simulated values $\mathbf{x}^{\mathcal{K}}(t_n)$ can be interpolated from $\mathbf{x}_{ij}$:

$$\begin{aligned} \mathbf{x}^{\mathcal{K}}(t_n) &= \sum_{j=0}^{\mathcal{K}} \ell_j(\tau_n)\ \mathbf{x}_{ij} \\ \text{for} \quad n &= 1, \ldots, \mathcal{M} \end{aligned} \tag{3.5}$$

where i and τ_n are selected for the appropriate finite element and sampling time. The objective function $\Phi(\mathbf{x}, \mathbf{p})$ is thus:

$$\Phi(\mathbf{x}, \mathbf{p}) = \sum_{n}^{\mathcal{M}} \left(\frac{\mathbf{x}^{\mathcal{K}}(t_n) - \hat{\mathbf{x}}(t_n)}{\boldsymbol{\text{œ}}_n} \right)^2 \tag{3.6}$$

where $\boldsymbol{\text{œ}}_n$ is the measurement error associated with measurement n. Since $\mathbf{x}$ and $\boldsymbol{\text{œ}}$ are vectors, the division in 3.6 must be performed element-wise. This cost function was taken from a similar multiple-shooting approach to parameter estimation [37].

Since the cost function (3.6) and equality constraints (3.2, 3.3, and 3.4) now satisfy continuity and differentiability requirements [38], parameter estimation can now be accomplished via constrained nonlinear programming (NLP) instead of a global search strategy. The solution is subject to variable bounds:

$$\begin{aligned} \mathbf{x}_{LB} \leq \mathbf{x} \leq \mathbf{x}_{UB} \\ \mathbf{p}_{LB} \leq \mathbf{p} \leq \mathbf{p}_{UB} \end{aligned} \tag{3.7}$$

The numerical implementation is accomplished using IPOPT [39], using the `MA57` [40] linear solver. The CasADi computer algebra package [**?**] was used to provide an interface to the IPOPT numerical libraries and supply derivatives to the cost and equality function calls through automatic differentiation.

3.2.2 Generating Initial Values

Solution of the NLP described in section 3.2.1 requires a suitable initial guess for the optimal state profiles, $\mathbf{x}^\star$, and kinetic parameters, $\mathbf{p}^\star$. To find approximate values for these variables, a smoothed periodic B-spline, $\tilde{\mathbf{x}}$, is found using experimental data for each state variable using SciPy's interpolate module [41]. Initial values for x_{ij} are obtained by evaluating this spline at each τ_k for each finite element.

$$\begin{aligned} & \mathbf{x}_{ij}^\star \approx \tilde{\mathbf{x}}(t_{ij}) \\ \text{where} \quad & t_{ij} = h(i-1+\tau_j) \\ \text{for} \quad & i = \{1,\ldots,\mathcal{N}\},\ j = \{1,\ldots,\mathcal{K}\} \end{aligned} \tag{3.8}$$

Since

$$\frac{d\tilde{\mathbf{x}}}{dt} \approx \mathbf{f}(\tilde{\mathbf{x}}, \mathbf{p}), \tag{3.9}$$

approximate values for $\mathbf{p}$ can be obtained by solving the simpler unconstrained NLP,

$$\min_{\mathbf{p}} \sum_{i}^{\mathcal{N}} \sum_{j}^{\mathcal{K}} \left(\frac{d\tilde{\mathbf{x}}(t_{ij})}{dt} - \mathbf{f}(\tilde{\mathbf{x}}(t_{ij}), \mathbf{p}) \right)^2 \tag{3.10}$$

in which t_{ij} is the same as in 3.8 and the bounds on p are the same as in 3.7.

3.2.3 First Order Sensitivity Analysis

After determining an optimal parameter set for the given experimental data, relevant first order sensitivity coefficients for oscillatory models are found using the procedure from [19], summarized here.

First, initial conditions and oscillatory period are verified by solving the boundary value problem (BVP):

$$\min_{\mathbf{x}(0),T} \begin{pmatrix} \mathbf{x}(T) - \mathbf{x}(0) \\ \dot{\mathbf{x}}_0(0) \end{pmatrix} \tag{3.11}$$

where $\dot{\mathbf{x}}_0(0)$ denotes the time-derivative of the first state variable, evaluated at $t = 0$. This BVP is solved using Newton's method, employing the SUNDIALS packages CVODES for ODE integration and KINSOL for the Newton iterations [18].

Time-dependent parametric sensitivities,

$$\mathbf{S}(t) \equiv \frac{\partial \mathbf{x}(t)}{\partial \mathbf{p}},$$

are obtained by using the staggered-direct method from the CVODES integrator [42]. Sensitivities of the period, $\frac{\partial T}{\partial \mathbf{p}}$, can be obtained directly from sensitivities integrated for one pass of the limit cycle (see [19] or [43] for further details) through a linear solve:

$$\begin{bmatrix} \mathbf{M} - \mathbf{I} & \dot{\mathbf{x}}(T) \\ \frac{\partial \mathbf{f}_0}{\partial \mathbf{x}}(\mathbf{x}(0)) & 0 \end{bmatrix} \begin{bmatrix} \vdots \\ \frac{\partial T}{\partial \mathbf{p}} \end{bmatrix} = \begin{bmatrix} -\mathbf{S}(T) \\ -\frac{\partial \mathbf{f}}{\partial \mathbf{p}}(\mathbf{x}(0)) \end{bmatrix} \tag{3.12}$$

in which $\mathbf{M}$ is the Monodromy matrix, $\mathbf{I}$ is the identity matrix, and the unknown vector contains the relevant period sensitivities.

Since parameter values often span several orders of magnitude, an often more useful measure is the relative period sensitivity, which is independent of the magnitude of the period or parameter value.

$$\frac{\partial \ln T}{\partial \ln \mathbf{p}} = \frac{\mathbf{p}}{T} \frac{\partial T}{\partial \mathbf{p}} = \frac{\partial T}{T} \Big/ \frac{\partial \mathbf{p}}{\mathbf{p}} \tag{3.13}$$

Thus, a relative period sensitivity of 1 indicates that a 1% increase in the parameter value will result in a 1% increase in the period.

3.2.4 Generation of data for bootstrap methods

For each run, two thousand simulated measurements, $\hat{x}_i(t_j)$, were generated from the true data, $\tilde{x}_i(t_j)$, using a normal distribution with $\mu = \tilde{x}_i(t_j)$ and $\sigma_{ij} = \xi\ \tilde{x}_i(t_j) +$

$\eta \ \max_j \tilde{x}_i(t_j)$, in which ξ is the relative and η is the absolute error. Each simulated data set was then used to find a unique optimum parameter set, $\mathbf{p}^\star$. Data sets that failed to converge, or reached a steady state solution (in which periodic sensitivities are undefined), were discarded from further analysis.

For the *in silico* data of varying quality used in Figures 2-4, we used the known limit cycle $\mathbf{x}(t)$ to generate data points $\hat{x}_i(t_j)$ at each of $\mathcal{M}$ sampling points. The effect of increasing error and decreasing number sampling points were tested independently:

$$\xi = \{.01, .05, .10, .20, .30\}; \quad \mathcal{M} = 20$$
$$\mathcal{M} = \{30, 20, 15, 10, 5\}; \qquad \xi = 0.15$$

Since standard deviations in the data distributions were also used as optimization weights, a small amount of absolute error ($\eta = 0.001$) was added to ensure errors in small values did not dominate the cost function.

3.2.5 Calculation Times

Each parameter estimation took approximately 4 seconds on a 2.53GHz processor, with the subsequent limit cycle solution integration and sensitivity calculation taking approximately 0.5 seconds. Due to the parallel nature of the 2000 trials, computation times were alleviated by distributing the tasks onto a cluster of 160 compute nodes.

3.2.6 Software

The numerical implementation of the nonlinear programming optimizations was accomplished using IPOPT [39]. The CasADi computer algebra package [**?**] was used to provide an interface to the IPOPT numerical libraries and supply derivatives to the cost and equality function calls through automatic differentiation.

Other libraries used were the SUNDIALS [18] packages CVODES for ODE integration and KINSOL for the Newton iterations involved in the solution of the limit cycle. Integration of the sensitivity equations was performed by using the staggered-direct method from the CVODES integrator.

3.3 Results and discussion

Mechanistic models of biological processes are often posed as nonlinear, time-invariant systems of ordinary differential equations (ODEs) [8, 9, 10], of the form:

$$\frac{d\mathbf{x}}{dt} = \mathbf{f}(\mathbf{x}(t), \mathbf{p}) \tag{3.14}$$

in which the vector of state variables $\mathbf{x}(t)$ describe the time-dependent activity of important species (i.e., mRNA, proteins, or metabolites), the parameters $\mathbf{p}$ are the kinetic rate constants, and the vector function $\mathbf{f}(\mathbf{x}(t), \mathbf{p})$ contains the transcription, translation, transport, and degradation rate laws of the gene regulatory network. In modeling rhythmic phenomena, we typically seek models and parameter values that display *limit cycle* oscillations - where for the solution approaches a non-trivial periodic trajectory:

$$\lim_{t\to\infty} \mathbf{x}(t) = \mathbf{x}(t+T). \tag{3.15}$$

Here the period of oscillation is the smallest $T > 0$ in which the equality (3.15) holds. Limit cycle oscillations are independent of the system's initial values $\mathbf{x}(0)$, and are instead determined completely by the parameters $\mathbf{p}$.

Experimental values for $\mathbf{p}$ are rarely available. Given time-series experimental measurements $\hat{x}_i(t_j)$ for each state variable in a limit cycle system, we find optimal parameters $\mathbf{p}^\star$ such that the error between the experimental measurements and the

simulated limit cycle is minimized [37]:,

$$\mathbf{p}^{\star} := \arg\min_{\mathbf{p}} \sum_{i}^{states} \sum_{j}^{data} \frac{\left(\hat{x}_i(t_j) - x_i(t_j, \mathbf{p})\right)^2}{\sigma_{ij}^2}. \tag{3.16}$$

Here σ_{ij} is the standard deviation associated with the measured mean of state i at time j. Using the data points $\hat{x}_i(t_j)$ to generate a suitable initial guess, parameter estimation may proceed via a nonlinear programming approach (see Methods). In this work, we assume that all states are measured to demonstrate how initial guesses can be generated directly from the input data. However, for systems with unmeasured states, initial guesses for the trajectory and parameter values can be provided by another approach, such as a global optimization routine. A bootstrap method was implemented by repeatedly sampling input data distributions to calculate a population of optimal parameter fits.

After finding optimal parameter fits, we used the models to predict how perturbations change systems dynamics by performing a first order sensitivity analysis. Since adjustments to periodic systems in response to inputs are often manifested through temporary changes in oscillatory period, relative period sensitivities,

$$\frac{\partial \ln T}{\partial \ln \mathbf{p}} \tag{3.17}$$

were calculated due to their independence of parameter magnitude [19, 43, 44]. Relative period sensitivities were integrated into the bootstrap method by calculating appropriate sensitivities for each estimated parameter set.

Of particular importance in determining the reliability of a model prediction is whether an output response maintains a consistent direction despite noise in measurement data. We therefore define a sensitivity value to be practically identifiable for given input data if 95% of the distribution maintains a consistent sign, similar to definitions for parameter identifiability used in previous studies [28, 45]. An overview

of the method is shown in Figure 1.

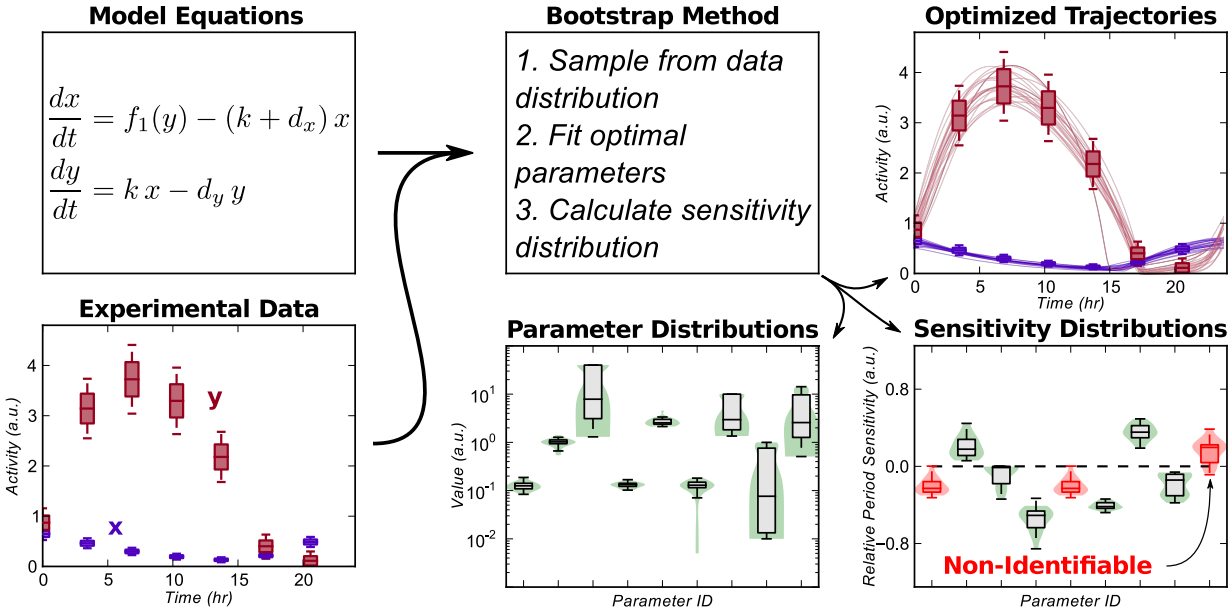

Figure 3.1: Parameter Estimation and Bootstrap Methods Flowchart. The demonstrated method calculates confidence intervals in the sensitivity of limit cycle models. An oscillatory model and experimental (or simulated) data are inputs to the bootstrap method. Unique data sets are then used to calculate optimum limit cycle trajectories. The resulting distribution in sensitivities highlight whether a particular response is identifiable (i.e., consistent across the majority of bootstrap trials.)

3.3.1 Effect of data quality on predictive confidence

We first analyze the degree to which uncertainty in input data is propagated to uncertainty in output predictions. To achieve this, we generate *in silico* data from a previously published model of circadian rhythms, using relative error ξ to generate normally distributed data ($\sigma_{ij} = \xi\ \hat{x}_i(t_j)$) at each of $\mathcal{M}$ sampling points. As expected, solution trajectories drifted further from the nominal limit cycle for higher values of error, ξ, or lower sampling density, $\mathcal{M}$, (Figure 2). However, the overall shape of the oscillatory profiles remained relatively similar, even for rather high ξ or low $\mathcal{M}$.

Figure 3 shows violin plots of the probability distribution for each parameter set and corresponding sensitivity evaluation for increasing ξ, while Figure 4 shows sim-

ilar plots for decreasing $\mathcal{M}$. Interestingly, there is little correlation between the identifiability of a parameter and its corresponding sensitivity value. For example, vdP, the maximum degradation rate of Per mRNA, shows a very tight clustering about its nominal parameter value, while the sensitivity of this parameter loses identifiability for even small values of ξ. Conversely, KdCn, the Michealis-Menten constant associated with the degradation of nuclear CRY, shows large variations in possible parameter values. However, the period sensitivity of KdCn, despite lying close to the x-axis, remains identifiable, indicating a robust prediction. These results reveal which model responses are constrained by the structure and dynamics of the limit cycle oscillations, and which are dependent on the particular parameterization chosen.

Sensitivities that are experimentally distinguishable from zero are the most important for validation. Calculating a typical experimental value for a relative period sensitivity helps to calibrate which sensitivities might be verified experimentally. Referring to a recent RNA interference screen, periods changes of approximately 1 hour (5%) can be reliably measured using luminescence recordings [4]. Assuming an increase in the corresponding mRNA degradation parameter value of 50%, this translates to a relative period sensitivity of 0.1. Thus, many of the identifiable values shown in Figures 3-4 fall within the experimentally measurable range.

3.3.2 Application to literature data for model discrimination

We next apply the method to literature time-course data for core clock components [11]. When modeling a genetic regulatory network, many candidate model equations are often considered. We show that a bootstrap uncertainty analysis can also be useful in discriminating between potential model structures based on predictive confidence. Here two variations of the same model are fit: The first model (Table 2.1) was originally optimized using a genetic algorithm approach, and thus contains a minimal

number of parameters to reduce optimization complexity. The second model (Table 3.1) considered contains independent parameters for each rate expression, increasing the number of parameters from 23 to 35.

Table 3.1: Model Equations for the Expanded Model. These equations have similar reaction stoichiometry to those in table 2.1, but with more parametric degrees of freedom. This model showed better time-series performance than the more constrained model when fit to time-series data.

$$\frac{d\mathbf{p}}{dt} = \frac{\mathsf{Vm1}}{1+\mathsf{Vm1}\left(\frac{\mathbf{C1N}+\mathbf{C2N}\ \mathsf{M1}}{\mathsf{Ki1}}\right)^3} - \frac{\mathsf{k1}\ \mathbf{p}}{1+\frac{\mathbf{p}}{\mathsf{Km1}}}$$

$$\frac{d\mathbf{c1}}{dt} = \frac{\mathsf{Vm2}}{1+\mathsf{Vm2}\left(\frac{\mathbf{C1N}+\mathbf{C2N}\ \mathsf{M2}}{\mathsf{Ki2}}\right)^3} - \frac{\mathsf{k2}\ \mathbf{c1}}{1+\frac{\mathbf{c1}}{\mathsf{Km2}}}$$

$$\frac{d\mathbf{c2}}{dt} = \frac{\mathsf{Vm3}}{1+\mathsf{Vm3}\left(\frac{\mathbf{C1N}+\mathbf{C2N}\ \mathsf{M3}}{\mathsf{Ki3}}\right)^3} - \frac{\mathsf{k3}\ \mathbf{c2}}{1+\frac{\mathbf{c2}}{\mathsf{Km3}}}$$

$$\frac{d\mathbf{P}}{dt} = \mathsf{k4}\ \mathbf{p} + \mathsf{k12}\ \mathbf{C1N} + \mathsf{k13}\ \mathbf{C2N} - \frac{\mathsf{k7}\ \mathbf{P}}{1+\frac{\mathbf{P}}{\mathsf{Km4}}} - \mathsf{k10}\ \mathbf{P}\ \mathbf{C1} - \mathsf{k11}\ \mathbf{P}\ \mathbf{C2}$$

$$\frac{d\mathbf{C1}}{dt} = \mathsf{k5}\ \mathbf{c1} + \mathsf{k12}\ \mathbf{C1N} - \frac{\mathsf{k8}\ \mathbf{C1}}{1+\frac{\mathbf{C1}}{\mathsf{Km5}}} - \mathsf{k10}\ \mathbf{P}\ \mathbf{C1}$$

$$\frac{d\mathbf{C2}}{dt} = \mathsf{k6}\ \mathbf{c2} + \mathsf{k13}\ \mathbf{C2N} - \frac{\mathsf{k9}\ \mathbf{C2}}{1+\frac{\mathbf{C2}}{\mathsf{Km6}}} - \mathsf{k11}\ \mathbf{P}\ \mathbf{C2}$$

$$\frac{d\mathbf{C1N}}{dt} = \mathsf{k10}\ \mathbf{P}\ \mathbf{C1} - \mathsf{k12}\ \mathbf{C1N} - \frac{\mathsf{k14}\ \mathbf{C1N}}{1+\frac{\mathbf{C1N}+\mathbf{C2N}\ \mathsf{M4}}{\mathsf{Km7}}}$$

$$\frac{d\mathbf{C2N}}{dt} = \mathsf{k11}\ \mathbf{P}\ \mathbf{C2} - \mathsf{k13}\ \mathbf{C2N} - \frac{\mathsf{k15}\ \mathbf{C2N}}{1+\frac{\mathbf{C1N}+\mathbf{C2N}\ \mathsf{M5}}{\mathsf{Km8}}}$$

The literature data used consisted of 7-8 concentration time points across a 24 hour period. Confidence intervals in the data were not available, so an optimistic 3% relative and 0.5% absolute error was assumed for each data point ($\sigma_{ij} = 0.03\ \hat{x}_i(t_j) + 0.005\ \max(\hat{x}_i)$). Figure 5A shows the resulting time-series profiles for bootstrap estimations of each model. While additional kinetic parameters are typically thought to lower the predictive confidence of a model (the 'curse of dimensionality'), the

expanded model is able to better capture the oscillatory profiles with lower variability between solutions. Parameter and sensitivity distributions, Figure 5B, similarly show how the expanded model parameterization is able to generate more confident predictions in model response. Since the resulting sensitivity identifiability for both models was relatively poor, we highlight sensitivities which pass a 90% confidence level threshold. These results thus indicate higher-resolution data on circadian components would help in conferring confidence to model predictions.

Two sensitivities, the PER translation rate (Figure 5B, 1) and the PER-CRY association rate (2), had high confidence and consistent direction in both the base and expanded parameterization - suggesting that the predicted values are robust to slight changes in both parameter value and model structure. Since a biological system can be modeled using many different combinations of kinetic assumptions, such a technique will likely prove useful in finding consistent predictions which are robust to slight differences in model equations.

Figure 6 compares optimal fits for both the base and expanded models to the originally published parameter set [30]. Since the original cost function was concerned mostly with optimizing stoichiometric and knockout data, the refitted models are able to much more accurately represent the time-series dynamics.

3.4 Conclusions

Increasingly, mathematical models are being used to study biological systems where traditional experiments would prove infeasible. For example, in the search for drug targets, thousands of possible combinatorial perturbations can be quickly scanned for therapeutic effects using *in silico* modeling. This is especially useful in oscillatory systems with long periods, such as circadian rhythms, where a perturbed *in vitro* or *in vivo* system must be measured for multiple days before changes can be reliably

determined.

However, since errors in model responses can arise from either incorrect structure or measurement noise, our confidence in *in silico* predictions is limited. Here we have developed a bootstrap approach suitable for periodic systems, and extended it to include uncertainty in predicted responses. With this method, errors due to local parameter effects can be identified, even in models with complicated dynamics. Furthermore, by considering multiple variations in model assumptions, we have demonstrated that a clearer result of trustworthy model predictions can be found.

Since this method takes advantage of time-series data to generate a strong initial guess for an otherwise difficult parameter estimation, it requires high-resolution data on the concentrations of all species in the model. In many biological systems, such data is only available for the activity levels of certain well-studied species. However, the continued development of high-throughput genomic and proteomic techniques promise to deliver time-series data for a much larger network of components. With expanding datasets, these methods will likely prove useful for the quantitative evaluation of uncertainty in larger biological models.

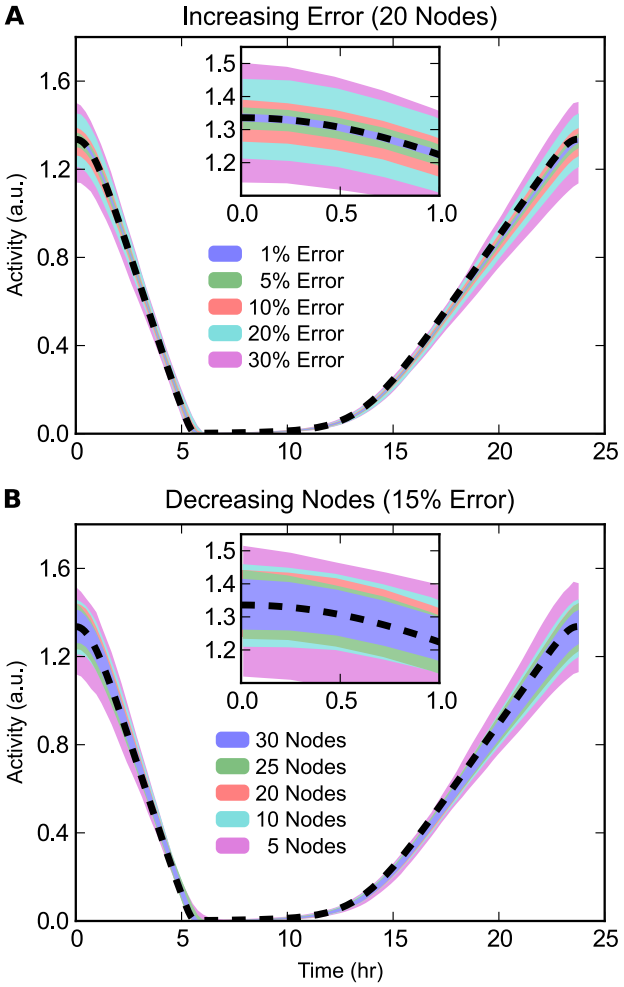

Figure 3.2: Time-course Profiles of the State Trajectories for Per mRNA. (A) Increasing relative error, ξ, with $\mathcal{M} = 20$. Possible state variable values are shown as shaded regions, obtained by filling between the 5^{th} and 95^{th} percentile for values at each time for 2000 independent parameter estimations. Increasing ξ results in larger deviations from the original model trajectory, shown as a dashed black line.
(B) Decreasing number of measurement points, $\mathcal{M}$, each with $\xi = 0.15$. Higher $\mathcal{M}$ results in trajectories closer to the true trajectory.

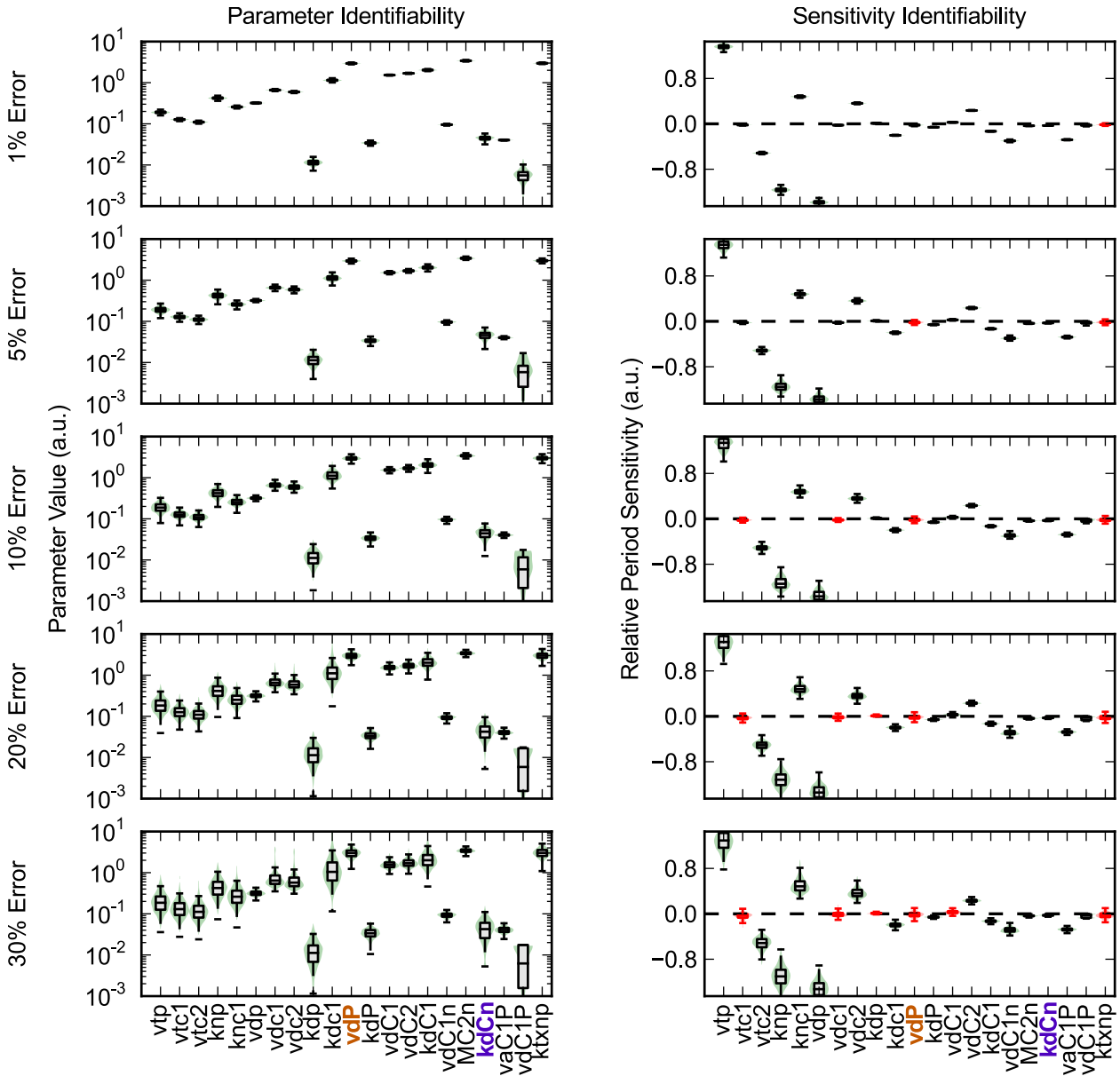

Figure 3.3: Parameter and Sensitivity Identifiability for Increasing Error. Increasing ξ results in a corresponding decrease in the confidence of the parameter and sensitivity estimates. Violin plots of the parameter values (left) and relative period sensitivities (right) show the distribution of values from each parameter estimation. In the plots, a box plot is superimposed above a kernel density plot to convey the distribution of values. The whiskers used extend to the most extreme data point within 1.5x the inner quartile range. Sensitivities in which the 5^{th} and 95^{th} percentile values span the x-axis are deemed non-identifiable (red), as the model's response direction can not be accurately estimated. Higher ξ also results in wider parameter distributions.

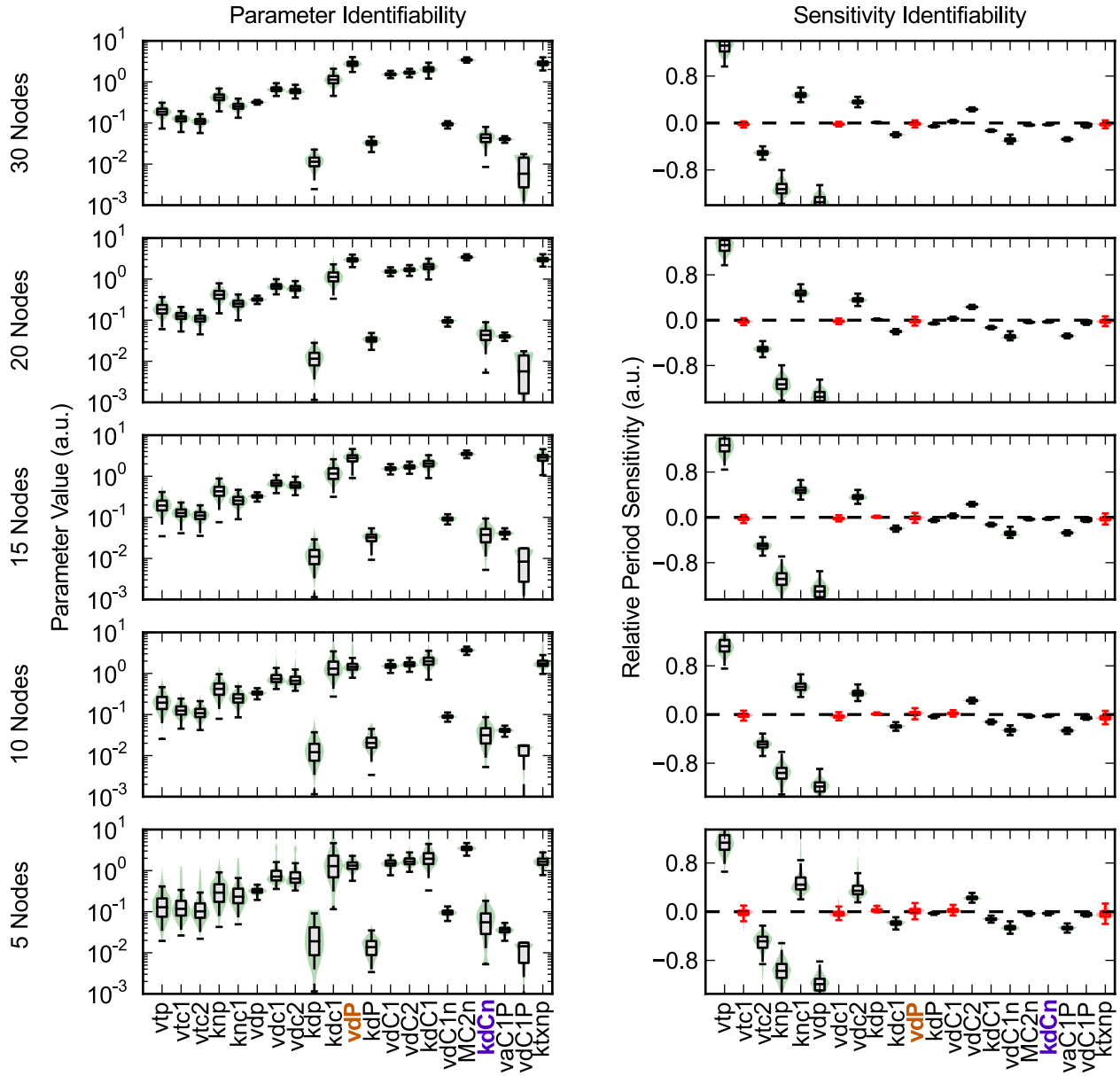

Figure 3.4: Effect of High-resolution Sampling on Identifiability. Lower values of $\mathcal{M}$ result in less constrained parameter and sensitivity values. Similar to Figure 3, violin plots of the parameters (left) and sensitivities (right) show the distribution from each parameter estimation for decreasing $\mathcal{M}$. These results highlight the importance of high-resolution time sampling in generating sensitivity information for oscillatory models.

Table 3.2: Parameter Set for Expanded Model. Parameters for model described in table 3.1, fit to time-series data via nonlinear programming.

	Parameter	Description	Value
1	M1	*Per*/CRY2 activity coefficient	3.632
2	Vm1	*Per* transcription rate	9.957×10^{-1}
3	Ki1	*Per*/CRY inhibition coefficient	1.054×10^{-1}
4	M2	*Cry1*/CRY2 activity coefficient	1.000×10^{-3}
5	Vm2	*Cry1* transcription rate	2.262×10^{-1}
6	Ki2	*Cry1*/CRY inhibition coefficient	2.049×10^{-1}
7	M3	*Cry2*/CRY2 activity coefficient	1.000×10^{1}
8	Vm3	*Cry2* transcription rate	1.850×10^{-1}
9	Ki3	*Cry2*/CRY inhibition coefficient	1.427×10^{-1}
10	k1	*Per* degradation rate	2.920×10^{-1}
11	Km1	*Per* degradation self-inhibition	6.609×10^{-1}
12	k2	*Cry1* degradation rate	1.000×10^{1}
13	Km2	*Cry1* degradation self-inhibition	1.823×10^{-2}
14	k3	*Cry2* degradation rate	4.711×10^{-2}
15	Km3	*Cry2* degradation self-inhibition	1.000×10^{1}
16	k4	*Per* translation rate	1.132×10^{-1}
17	k5	*Cry1* translation rate	3.409×10^{-1}
18	k6	*Cry2* translation rate	1.961×10^{-1}
19	k7	PER degradation rate	1.000×10^{1}
20	Km4	PER degradation self-inhibition	1.911×10^{-3}
21	k8	CRY1 degradation rate	1.000×10^{1}
22	Km5	CRY1 degradation self-inhibition	2.077×10^{-2}
23	k9	CRY2 degradation rate	1.000×10^{1}
24	Km6	CRY2 degradation self-inhibition	1.180×10^{-2}
25	k10	C1N association rate	5.022×10^{-1}
26	k11	C2N association rate	1.035
27	k12	C1N dissociation rate	1.000×10^{-3}
28	k13	C2N dissociation rate	2.070×10^{-1}
29	M4	CRY1n/CRY2n activity coefficient	1.000×10^{1}
30	k14	CRY1N degradation rate	1.000×10^{1}
31	Km7	CRY1n degradation inhibition	5.206×10^{-3}
32	M5	CRY2n/CRY2n activity coefficient	1.000×10^{1}
33	k15	CRY2n degradation rate	1.000×10^{1}
34	Km8	CRY2n degradation inhibition	1.829×10^{-2}

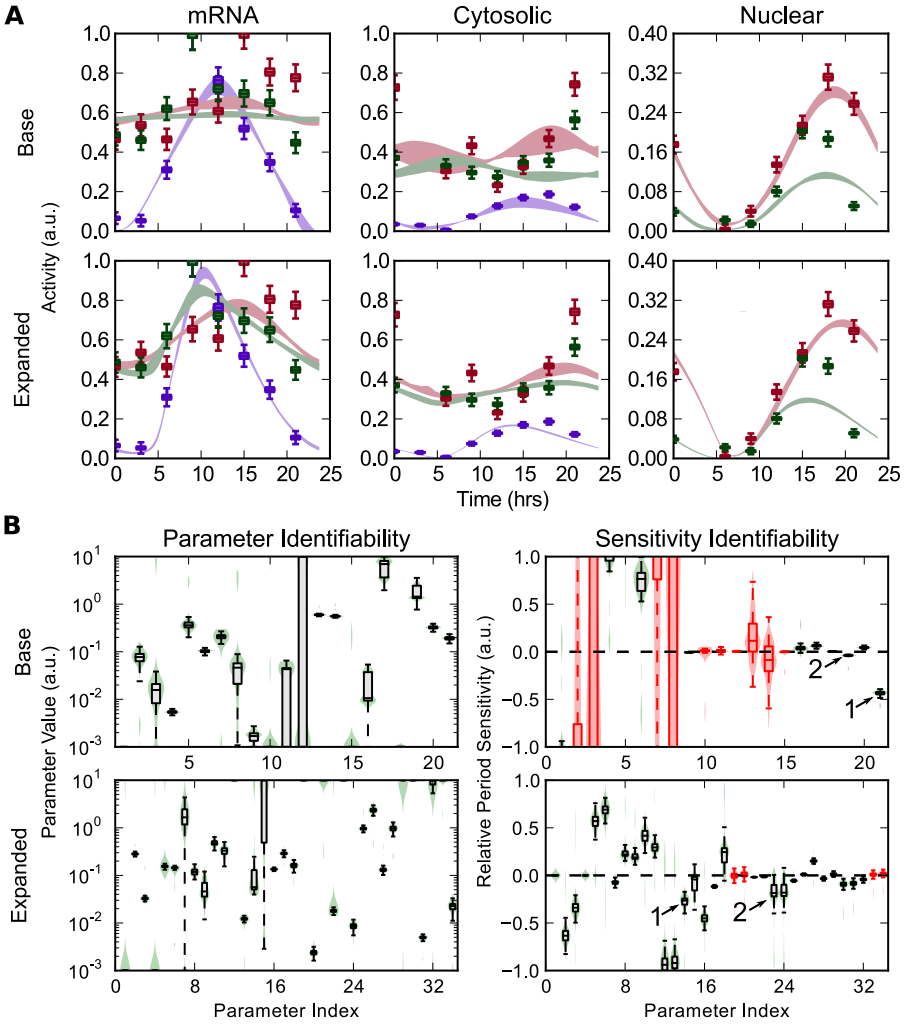

Figure 3.5: Identifiability Comparison of Two Model Structures. (A) Bootstrap parameter estimations on two model structures using literature time-series data with estimated errors (box plots). Resulting regions of model trajectories are shaded between the 5th and 95th percentile. *Per* species are shown in purple, *Cry1* in red, and *Cry2* in green. While both models were able to approximately reproduce the same dynamic response, the expanded model was better able to capture differences between the *Cry1* and *Cry2* profiles. (B) Parameter and sensitivity identifiability for the base and expanded models. Violin plots show the parameter and sensitivity distributions, with unidentifiable sensitivities (90% confidence level) highlighted in red. Despite containing more parameters, the expanded model shows better parameter identifiability and higher confidence in its predicted sensitivities. The PER translation rate (1) and PER-CRY association rate (2) sensitivities are consistent across model equations and are highlighted.

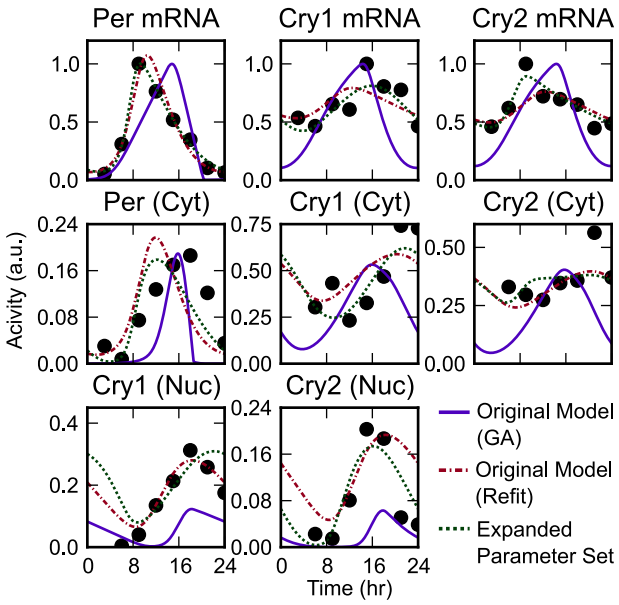

Figure 3.6: Time-Series Dynamics of Fitted Models. Model trajectories for each of the considered models. The original model (purple) shows the time series dynamics for the previously published parameter set, used in Figures 1-4. In these plots, the original model's period and amplitudes were rescaled to best match the experimental data, shown in black (without changing the dynamic profiles). The refitted model (red, dashed) was generated by optimizing the dynamic profile to time series data using the parameter estimation routine described in Supplemental Text 1. The expanded model (green, dashed) consists of a similar network structure, but with independent kinetic parameters for each rate expression (see Supplemental Text 2). These plots show that parameter optimization through nonlinear programming is able to more accurately fit gene and protein expression profiles.

Chapter 4

Spatiotemporal separation of PER and CRY posttranslational regulation

4.1 Introduction

Circadian rhythms are autonomous, near-24 hour oscillations that coordinate daily changes in physiology and metabolism. Since circadian and metabolic regulators are tightly integrated, circadian disruptions often manifest in metabolic disease [46]. Recent efforts have therefore sought to gain a mechanistic understanding of these pathways, such that the metabolic burdens imposed by a 24-hour society might be mitigated. Post-translational regulators, which play key roles in connecting circadian and metabolic processes, serve as likely targets for future therapeutics – demonstrated by the wealth of available circadian-active small molecules [47].

Oscillations in circadian gene transcription are generated through a time-delayed transcription-translation negative-feedback loop. In mammals, transcription factors CLOCK and BMAL1 promote transcription of E box-containing genes *Period* (*Per*) and *Cryptochrome* (*Cry*) (Fig. 1A). PER and CRY protein products form heterodimers to accumulate in the nucleus, in which PER is stoichiometrically limiting [11], and sub-

sequently close the negative feedback loop by inhibiting CLOCK-BMAL1-promoted gene expression. While steady-state endpoint assays have shown the possibility of nuclear entry of CRY without PER [7, 48, 49], experiments from *Per1*$^{-/-}$ *Per2*$^{-/-}$ mice demonstrated that PER proteins are required for the timely nuclear accumulation of CRY [11]. Clearance of nuclear repressors reactivates CLOCK-BMAL1, allowing the cycle to begin anew [50].

Experimental evidence on PER/CRY nuclear entry is seemingly contradictory. For nuclear localization of the PER and CRY proteins, experiments from *Per1*$^{-/-}$ *Per2*$^{-/-}$ mice demonstrate that PER proteins are required for timely nuclear accumulation of CRY [11]. While other studies have shown the possibility of nuclear entry of CRY without PER, these results are typically based on steady-state endpoint assays which do not consider the speed of CRY nuclear entry [7, 48, 49]. We therefore consider the formation of the PER-CRY heterodimer as a key step in nuclear entry, which is supported by the fact that to the best of our knowledge all circadian models that consider both PER and CRY employ this kinetic assumption [8, 9, 10, 20, 30].

The stabilities of PER and CRY are tightly regulated: PER proteins are phosphorylated by the casein kinase I family of proteins (CKIδ/ϵ), prompting β-TrCP-mediated degradation [51] and nuclear import [52]. The degradation of CRY proteins is separately regulated by the SCF$^{\text{FBXL3}}$ ubiquitin ligase complex [53, 54, 55]. The activities of both CKI-PER and FBXL3-CRY may be further coupled to the cell's metabolic state through AMPK signalling [56]. These post-translational regulatory mechanisms have a strong effect on period length: the gain-of-function mutant CKIϵ^{tau} leading to hyperphosphorylation of PER [57] and small molecule CKI inhibitors, such as longdaysin [34], demonstrated that increasing or decreasing CKI-dependent PER phosphorylation shortens or lengthens the period, respectively. In contrast, genetic mutations of FBXL3 [54, 55] and KL001, a small molecule inhibitor of FBXL3-dependent CRY degradation [30], showed that increased CRY stability leads to longer periods.

Since the scale and complexity of the circadian network complicates an intuitive understanding of these relationships, mathematical models have played important roles in understanding how these manipulations affect circadian period [30, 51, 57].

Given that both CKI and FBXL3 pathways regulate the stability of linked negative factors, it was thought that simultaneous perturbations to both pathways might lead to non-additive effects: *i.e.*, the slowest link would determine the period. However, both small molecule [30] and genetic experiments [58] have demonstrated the independent period effects of these two post-translational regulations. A recent clarification of the canonical clock feedback circuit has shown that dissociated CRY is the dominant repressor of CLOCK-BMAL1 mediated E box transcription [48]. This distinction helps differentiate between the roles of the otherwise similar PER and CRY proteins, in which the main role of PER in transcriptional repression is likely regulating the timing of nuclear accumulation of CRY. Therefore, while previous mathematical models in which PER acts as a direct repressor have proposed mechanisms for CKI-dependent period lengthening [57, 59], they are likely not suitable for distinguishing between CKI-PER and FBXL3-CRY mediated period change.

In this study, we used human cells harboring clock gene reporters together with mathematical modeling to gain insight into the relationship between PER and CRY post-translational regulation. Consequently, we provide a new mechanism by which CKI-dependent PER phosphorylation controls the circadian period separately from the FBXL3-CRY pathway. The resulting detailed understanding of PER and CRY regulation in the core feedback loop provides a framework on which to interpret metabolic and pharmacological control of circadian rhythms.

4.2 Materials and Methods

4.2.1 Analysis of luminescence profiles

Raw luminescence data was first separated into a moving baseline and oscillatory component using a Hodrick-Prescott filter with a smoothing parameter of 1600. Example trajectory decompositions are shown in Figure S1. Amplitudes (as shown in Fig. 1C) were determined by taking the standard deviation in the baseline-subtracted data. Periods were obtained by nonlinear curve fitting, in which a four parameter (initial amplitude, decay, period and phase) damped cosine curve was fit to the baseline-subtracted data. Periods were not shown if the relative amplitude (found by standard deviation) fell below 25%, since noise dominated the periodic trajectory.

4.2.2 Cost function

Models were fit to a cost function of experimental results. *Per*, *Cry*, *Clock*, and *Bmal1* protein and mRNA levels were taken from [11], along with profiles of CRY nuclear localization. For the model from [20], additional activity profiles on *Rev-Erb* and *Ror* were obtained from CircaDB (http://bioinf.itmat.upenn.edu/circa/). To score a model trajectory, mRNA state variables were scaled independently to minimize the squared error between model and experiment, since model parameters could be adjusted to give mRNA profiles arbitrary amplitudes. For protein species, where stoichiometric interactions are important, a single scaling parameter was used for all species. Nuclear repressor species, in which only relative measurements were available, were scaled independently. Full model equations are shown in the SI.

4.2.3 Parameter estimation and bootstrap analysis

Bootstrap parameter estimations were performed as described previously [60], with data from [11] assumed to have a normally distributed 10% relative and 5% absolute error. Since not all states in the models were measured, initial guess values for the trajectory and parameter variables were generated by optimizing the parameter sets first with a genetic algorithm approach, described in [9]. To help ensure bootstrap trials remained in a similar stability region of parameter space (and protect against steady-state solutions), bootstrap parameters were bound between 50% and 150% of their initial value.

4.2.4 Selection of parameters for FBXL3-CRY and CKI-PER mechanisms

For FBXL3-CRY, parameters that determined the degradation rate of CRY (or CRY containing complexes) were considered to be the most likely candidates. Michealis-Menten degradation parameters were omitted from Fig. 3 since perturbations to such parameters are not easily attributable to changes in FBXL3 binding affinity. In the model presented in [8], CRY is degraded through a series of phosphorylation events, and these parameters were considered as representative of the rate of progression toward ubiquitination of CRY. The forward phosphorylation rates of CRY and nuclear PER-CRY complex were therefore also considered. For CKI-PER, we considered rates that determined the degradation rate and nuclear import rate of PER. Michealis-Menten parameters were not included, similar to FBXL3-CRY. With CRY being the main repressor of E box transcription [48], the degradation rates of PER-CRY complex were not considered as potential mechanisms of CKI. In the models of [8] and [20], the nuclear entry of PER-CRY requires two independent steps: the formation of the PER-CRY complex and the subsequent import of the complex. Therefore, the forward

reaction rates of each of these steps were included.

4.2.5 Numerical experiments

Numerical parameter inhibitions were performed by recalculating the limit cycle trajectory for each new parameter set to a tolerance of 10^{-8}, using computational methods described previously [19].

4.3 Results and Discussion

4.3.1 Longdaysin and KL001 yield opposite effects on the amplitude of circadian reporter expression

To gain a more detailed understanding of the roles of CKI-PER and FBXL3-CRY pathways, we applied small molecule compounds longdaysin and KL001, which cause stabilization of PER and CRY, respectively [30, 34] (Fig. 1A). We used *Bmal1*- and *Per2-dLuc* as circadian reporters, which represent different loops of the core clock mechanism and show circadian luminescence rhythms with mutually opposite phase. Time-course data on circadian reporter expression under increasing concentrations of longdaysin and KL001 [30] was analyzed for period and amplitude change (Figs. 1B, 1C, S1). Longdaysin caused dose-dependent increases in period and detrended amplitude to $\approx$ 50% of control values in both *Bmal1*- and *Per2-dLuc* reporter cells. In contrast, KL001 induced a simultaneous increase in period and strong reduction in amplitude. Modulation of the activity of CKI-PER and FBXL3-CRY is therefore differentiated by an opposite amplitude response.

4.3.2 Bootstrap approach reveals main period-determining perturbations

We next used *in silico* modeling to gain mechanistic insight into CKI-PER and FBXL3-CRY mediated circadian regulation. We previously described the connection between inhibition of FBXL3-dependent CRY degradation and period change [30]: increasing the stability of nuclear CRY results in longer transcriptional repression and increased period length. However, while CKI has been linked to modulating PER stability and nuclear entry, it remained unclear which perturbation dominates the period effect, and whether these processes are sufficient to separate the effects of CKI and FBXL3.

To generate predictions that are consistent across slight differences in model assumptions, we chose three mathematical models from the literature based on their moderate size and similar scope [8, 20, 30]. The models included, at a minimum, the expression and nuclear entry mechanisms of PER and CRY. We considered the formation of the PER-CRY heterodimer as a key step in nuclear entry, which is supported by the fact that, to the best of our knowledge, all circadian models that consider both PER and CRY employ this kinetic assumption [8, 9, 10, 20, 30].

Since dynamic models of genetic regulatory networks typically suffer from poor parameter identifiability [61], we demonstrate that our predictions are parameter-independent by employing a bootstrap identifiability analysis [60]. As part of the bootstrap method, the models were re-fit to experimental data [11] while ensuring appropriate protein stoichiometry. The state trajectories of the resulting 2000 parameter sets for each model are shown in Fig. 2, with reasonable agreement between models and experiment.

A first-order period sensitivity analysis, performed on each of the parameter sets, identified which parameters associated with PER and CRY protein activity had the greatest effect on period (Fig. S2). To simplify analysis, we present only those parameters that are associated with experimentally supported mechanisms of CKI and

FBXL3 in Fig. 3. We first tested parameters associated with potential FBXL3-CRY activity (Fig. 3A) to evaluate if our method matched the experimentally verified effect of KL001 [30]. Since CRY is the dominant repressor of CLOCK-BMAL1 [48], we attribute degradation rates of the PER-CRY complex to be representative of CRY clearance rates. We found that only parameters governing nuclear CRY degradation show a period lengthening effect upon inhibition, while rates associated with cytoplasmic CRY degradation show period shortening effects. These results match with our previous assertion that period lengthening occurs via nuclear CRY stabilization [30]. Experimental evidence has also indicated cytoplasmic CRY stabilization may lead to period shortening [14], a result consistent with our mathematical results.

We next describe parameters potentially associated with CKI-dependent regulation of PER localization and stability (Fig. 3B). Since PER is rate-limiting in the formation of the PER-CRY complex [11], rates associated with complex formation or nuclear import were included in this analysis. Conversely, we did not include degradation rates of PER-CRY nuclear repressive complex, since CRY alone is considered the main repressor. While it was hypothesized in models where PER acts as a direct repressor that the regulation of PER stability would play the dominant role determining the period [57, 59], our new assumptions revealed that parameters governing PER degradation showed only non-identifiable responses. However, inhibition of rates associated with the nuclear entry of the PER-CRY complex showed strong period lengthening effects. These results indicate that under our current understanding of clock kinetics, the regulation of nuclear import likely plays the prominent role in CKI-dependent period regulation.

4.3.3 Mathematical insights into the different and independent mechanisms of PER and CRY regulation

Using the model and parameter set of Hirota *et al.*, 2012 [30] and the perturbations identified in Fig. 3, we first confirmed that inhibition of nuclear CRY degradation (vdCn) and PER-CRY nuclear import (vaC1P) reproduced the experimental period and amplitude effects of the small molecules KL001 and longdaysin, respectively (Fig. 4A, compare with Fig. 1C). Comparison of the oscillatory profiles of *Per* mRNA and nuclear CRY protein (Fig. 4B) revealed that inhibition of FBXL3-dependent CRY degradation caused lingering nuclear CRY to not be completely purged each cycle. This excess repressor during the accumulating phase of *Per* and *Cry* transcripts resulted in lower E box amplitudes, providing a likely explanation for the effect of KL001.

In contrast, stabilization of cytoplasmic PER (lowering vdP) resulted in reduced transcriptional amplitude with minimal period effect (Fig. S3), consistent with experimental findings from the knockdown of β-TrCP, an F box protein responsible for PER degradation [62]. However, other experimental results have shown that down-regulation of β-TrCP leads to longer periods [51], suggesting that further modeling and experimental inquiry is needed on the role of β-TrCP in clock regulation. This period lengthening might be explained through β-TrCP-mediated stabilization of nuclear PER-CRY or by using alternative kinetic assumptions for the rate of PER-CRY binding.

We further compared the effect of inhibiting PER degradation with inhibiting nuclear import on the oscillatory profile of key clock proteins (Fig. 4C) to identify mechanistic differences between the two potential effects of CKI inhibition. Both perturbations increased cytoplasmic PER, suggesting the two mechanisms are difficult to distinguish experimentally. Direct stabilization of PER in the cytoplasm (lowering vdP) lead to two simultaneous trends which shift the period in opposite directions:

it shortened the time delay between transcription and inactivation by accelerating the accumulation of cytoplasmic PER and nuclear PER-CRY; and lengthened the repressive phase by increasing the total amount of PER-CRY which enters the nucleus. These perturbations sped and slowed the clock, respectively, and resulted in little period change. In contrast, inhibiting PER-CRY nuclear entry (lowering vaC1P) caused additional free protein to build in the cytoplasm, delaying nuclear accumulation and ultimately increasing the total amount of nuclear PER-CRY. Since both of these trends work to increase period length, inhibiting PER-CRY nuclear entry resulted in significantly longer cycles. Additionally, the longer cytoplasmic time delay resulted in increased transcription, yielding slightly higher amplitudes (Fig. 4B) that closely match the experimental results of the small molecule longdaysin.

Since CKI likely regulates both stability and subcellular localization of PER *in vivo*, we considered the effects of simultaneously lowering both PER cytoplasmic degradation and nuclear entry rates (Fig. 5A). The loss of oscillations under extreme reduction of both parameters (Fig. 5A, shaded regions) highlights an interesting role of CKI in conferring robustness to the circadian clock: since oscillations are lost when import of the PER-CRY complex to the nucleus ceases to be rhythmic, CKI ensures lingering PER is purged from the cytoplasm by one pathway or another before E box transcription resumes. This importance has been proven experimentally, as disruption of CKI-mediated regulation leads to compromised circadian oscillations [63].

Together, inhibition of CKI by longdaysin may increase the time required before PER-CRY can enter the nucleus to repress transcription, leading to a higher amplitude and longer period. In contrast, KL001 lengthens the period by stabilizing nuclear CRY, resulting in a longer time delay before transcription resumes and lower amplitude from increased E box repression. PER regulation through CKI is therefore partitioned to the accumulating phase, controlling the speed and amount of

PER-CRY complex that enters the nucleus. CRY regulation through FBXL3 is partitioned independently to the repressive phase, controlling the length of time until CLOCK-BMAL1-dependent transcription resumes (Fig. 6). This independence was reproduced *in silico* by the simultaneous reduction of nuclear CRY degradation and PER-CRY nuclear import (Fig. 5B), where nonlinear interactions in amplitude and period between the two perturbations are all but absent.

4.3.4 Conclusion

An understanding of the interactions between post-translational regulators is crucial for the further development of circadian pharmacological reagents, as efficient modulation of clock function will assuredly come from simultaneous perturbations to many connected species. In this study, we used circadian reporter cells together with mathematical modeling to provide mechanistic insight into the differences of CKI- and FBXL3- mediated post-translational regulation of PER and CRY. As a result, we clarified a process by which CKI exerts control over the circadian period, demonstrated through both the hyperphosphorylating CKIϵ^{tau} mutant and small molecule CKI inhibitors, such as longdaysin. In developing our predictions, we have used multiple models and parameterizations to ensure our mechanisms are consistent across many *in silico* realizations. These results reinforce the notion that computational modeling is essential in interpreting results in systems with complicated oscillatory feedback. Additionally, *in silico* analyses reveal hidden design principles of biological networks, as this work highlights the importance of the CKI family of kinases in conferring robustness to the circadian cycle.

Chapter 5

Amplitude metrics for cellular bioluminescence reporters

5.1 Motivation, link to previous chapter

Hello, here is some text without a meaning. This text should show what a printed text will look like at this place. If you read this text, you will get no information. Really? Is there no information? Is there a difference between this text and some nonsense like “Huardest gefburn”? Kjift – not at all! A blind text like this gives you information about the selected font, how the letters are written and an impression of the look. This text should contain all letters of the alphabet and it should be written in of the original language. There is no need for special content, but the length of words should match the language.

5.1.1 Different enzymes control circadian rhythms at different phases

Hello, here is some text without a meaning. This text should show what a printed text will look like at this place. If you read this text, you will get no information. Really? Is there no information? Is there a difference between this text and some

nonsense like “Huardest gefburn”? Kjift – not at all! A blind text like this gives you information about the selected font, how the letters are written and an impression of the look. This text should contain all letters of the alphabet and it should be written in of the original language. There is no need for special content, but the length of words should match the language.

5.1.2 Perturbations likely have a time-dependent effect on amplitude

Hello, here is some text without a meaning. This text should show what a printed text will look like at this place. If you read this text, you will get no information. Really? Is there no information? Is there a difference between this text and some nonsense like “Huardest gefburn”? Kjift – not at all! A blind text like this gives you information about the selected font, how the letters are written and an impression of the look. This text should contain all letters of the alphabet and it should be written in of the original language. There is no need for special content, but the length of words should match the language.

5.1.3 Comparison of Ukai vs Pulivarthy 2007

Hello, here is some text without a meaning. This text should show what a printed text will look like at this place. If you read this text, you will get no information. Really? Is there no information? Is there a difference between this text and some nonsense like “Huardest gefburn”? Kjift – not at all! A blind text like this gives you information about the selected font, how the letters are written and an impression of the look. This text should contain all letters of the alphabet and it should be written in of the original language. There is no need for special content, but the length of words should match the language.

5.2 Single cell amplitude metrics

Hello, here is some text without a meaning. This text should show what a printed text will look like at this place. If you read this text, you will get no information. Really? Is there no information? Is there a difference between this text and some nonsense like “Huardest gefburn”? Kjift – not at all! A blind text like this gives you information about the selected font, how the letters are written and an impression of the look. This text should contain all letters of the alphabet and it should be written in of the original language. There is no need for special content, but the length of words should match the language.

5.2.1 Definition of amplitude metric

Hello, here is some text without a meaning. This text should show what a printed text will look like at this place. If you read this text, you will get no information. Really? Is there no information? Is there a difference between this text and some nonsense like “Huardest gefburn”? Kjift – not at all! A blind text like this gives you information about the selected font, how the letters are written and an impression of the look. This text should contain all letters of the alphabet and it should be written in of the original language. There is no need for special content, but the length of words should match the language.

5.2.2 Finite difference ARC

Hello, here is some text without a meaning. This text should show what a printed text will look like at this place. If you read this text, you will get no information. Really? Is there no information? Is there a difference between this text and some nonsense like “Huardest gefburn”? Kjift – not at all! A blind text like this gives you information about the selected font, how the letters are written and an impression of

the look. This text should contain all letters of the alphabet and it should be written in of the original language. There is no need for special content, but the length of words should match the language.

5.2.3 Derivation of sensitivity-based method

Hello, here is some text without a meaning. This text should show what a printed text will look like at this place. If you read this text, you will get no information. Really? Is there no information? Is there a difference between this text and some nonsense like “Huardest gefburn”? Kjift – not at all! A blind text like this gives you information about the selected font, how the letters are written and an impression of the look. This text should contain all letters of the alphabet and it should be written in of the original language. There is no need for special content, but the length of words should match the language.

5.3 Population-level models

Hello, here is some text without a meaning. This text should show what a printed text will look like at this place. If you read this text, you will get no information. Really? Is there no information? Is there a difference between this text and some nonsense like “Huardest gefburn”? Kjift – not at all! A blind text like this gives you information about the selected font, how the letters are written and an impression of the look. This text should contain all letters of the alphabet and it should be written in of the original language. There is no need for special content, but the length of words should match the language.

5.3.1 Definitions and diffusion-convection equation

Hello, here is some text without a meaning. This text should show what a printed text will look like at this place. If you read this text, you will get no information. Really? Is there no information? Is there a difference between this text and some nonsense like “Huardest gefburn”? Kjift – not at all! A blind text like this gives you information about the selected font, how the letters are written and an impression of the look. This text should contain all letters of the alphabet and it should be written in of the original language. There is no need for special content, but the length of words should match the language.

5.3.2 Circular statistics

Hello, here is some text without a meaning. This text should show what a printed text will look like at this place. If you read this text, you will get no information. Really? Is there no information? Is there a difference between this text and some nonsense like “Huardest gefburn”? Kjift – not at all! A blind text like this gives you information about the selected font, how the letters are written and an impression of the look. This text should contain all letters of the alphabet and it should be written in of the original language. There is no need for special content, but the length of words should match the language.

5.3.3 Inverting $p(\theta, \hat{t})$

Hello, here is some text without a meaning. This text should show what a printed text will look like at this place. If you read this text, you will get no information. Really? Is there no information? Is there a difference between this text and some nonsense like “Huardest gefburn”? Kjift – not at all! A blind text like this gives you information about the selected font, how the letters are written and an impression of

the look. This text should contain all letters of the alphabet and it should be written in of the original language. There is no need for special content, but the length of words should match the language.

5.3.4 Calculating $\bar{x}(\hat{t})$ and $\hat{x}(\hat{t})$

Hello, here is some text without a meaning. This text should show what a printed text will look like at this place. If you read this text, you will get no information. Really? Is there no information? Is there a difference between this text and some nonsense like “Huardest gefburn”? Kjift – not at all! A blind text like this gives you information about the selected font, how the letters are written and an impression of the look. This text should contain all letters of the alphabet and it should be written in of the original language. There is no need for special content, but the length of words should match the language.

Chapter 6

Decay rate as proxy for cellular noise

Chapter 7

Conclusions and future work

7.1 Continuation of collaboration with Andrew

Hello, here is some text without a meaning. This text should show what a printed text will look like at this place. If you read this text, you will get no information. Really? Is there no information? Is there a difference between this text and some nonsense like "Huardest gefburn"? Kjift – not at all! A blind text like this gives you information about the selected font, how the letters are written and an impression of the look. This text should contain all letters of the alphabet and it should be written in of the original language. There is no need for special content, but the length of words should match the language.

7.1.1 Experimental validation of model predictions

Hello, here is some text without a meaning. This text should show what a printed text will look like at this place. If you read this text, you will get no information. Really? Is there no information? Is there a difference between this text and some nonsense like "Huardest gefburn"? Kjift – not at all! A blind text like this gives you information about the selected font, how the letters are written and an impression of

the look. This text should contain all letters of the alphabet and it should be written in of the original language. There is no need for special content, but the length of words should match the language.

7.1.2 Prediction of fasting perturbations

Hello, here is some text without a meaning. This text should show what a printed text will look like at this place. If you read this text, you will get no information. Really? Is there no information? Is there a difference between this text and some nonsense like “Huardest gefburn”? Kjift – not at all! A blind text like this gives you information about the selected font, how the letters are written and an impression of the look. This text should contain all letters of the alphabet and it should be written in of the original language. There is no need for special content, but the length of words should match the language.

small-molecule activators of SIRT1

Hello, here is some text without a meaning. This text should show what a printed text will look like at this place. If you read this text, you will get no information. Really? Is there no information? Is there a difference between this text and some nonsense like “Huardest gefburn”? Kjift – not at all! A blind text like this gives you information about the selected font, how the letters are written and an impression of the look. This text should contain all letters of the alphabet and it should be written in of the original language. There is no need for special content, but the length of words should match the language.

7.1.3 Validity of step vs pulse perturbation

Hello, here is some text without a meaning. This text should show what a printed text will look like at this place. If you read this text, you will get no information. Really? Is there no information? Is there a difference between this text and some nonsense like “Huardest gefburn”? Kjift – not at all! A blind text like this gives you information about the selected font, how the letters are written and an impression of the look. This text should contain all letters of the alphabet and it should be written in of the original language. There is no need for special content, but the length of words should match the language.

Characterization of insulin effect

Hello, here is some text without a meaning. This text should show what a printed text will look like at this place. If you read this text, you will get no information. Really? Is there no information? Is there a difference between this text and some nonsense like “Huardest gefburn”? Kjift – not at all! A blind text like this gives you information about the selected font, how the letters are written and an impression of the look. This text should contain all letters of the alphabet and it should be written in of the original language. There is no need for special content, but the length of words should match the language.

7.2 Amplitude maximization through therapeutic treatment

Hello, here is some text without a meaning. This text should show what a printed text will look like at this place. If you read this text, you will get no information. Really? Is there no information? Is there a difference between this text and some

nonsense like “Huardest gefburn”? Kjift – not at all! A blind text like this gives you information about the selected font, how the letters are written and an impression of the look. This text should contain all letters of the alphabet and it should be written in of the original language. There is no need for special content, but the length of words should match the language.

7.2.1 Optimal control strategies to maximize peripheral clock amplitude

Hello, here is some text without a meaning. This text should show what a printed text will look like at this place. If you read this text, you will get no information. Really? Is there no information? Is there a difference between this text and some nonsense like “Huardest gefburn”? Kjift – not at all! A blind text like this gives you information about the selected font, how the letters are written and an impression of the look. This text should contain all letters of the alphabet and it should be written in of the original language. There is no need for special content, but the length of words should match the language.

7.2.2 Fewest treatments, combinatorial perturbations, etc.

Hello, here is some text without a meaning. This text should show what a printed text will look like at this place. If you read this text, you will get no information. Really? Is there no information? Is there a difference between this text and some nonsense like “Huardest gefburn”? Kjift – not at all! A blind text like this gives you information about the selected font, how the letters are written and an impression of the look. This text should contain all letters of the alphabet and it should be written in of the original language. There is no need for special content, but the length of words should match the language.

7.3 Iterative optimization of network topology

Hello, here is some text without a meaning. This text should show what a printed text will look like at this place. If you read this text, you will get no information. Really? Is there no information? Is there a difference between this text and some nonsense like “Huardest gefburn”? Kjift – not at all! A blind text like this gives you information about the selected font, how the letters are written and an impression of the look. This text should contain all letters of the alphabet and it should be written in of the original language. There is no need for special content, but the length of words should match the language.

7.3.1 (Idea from Mitsubishi proposal)

Hello, here is some text without a meaning. This text should show what a printed text will look like at this place. If you read this text, you will get no information. Really? Is there no information? Is there a difference between this text and some nonsense like “Huardest gefburn”? Kjift – not at all! A blind text like this gives you information about the selected font, how the letters are written and an impression of the look. This text should contain all letters of the alphabet and it should be written in of the original language. There is no need for special content, but the length of words should match the language.

7.3.2 Design machine-learning algorithm to find optimum model structure

Hello, here is some text without a meaning. This text should show what a printed text will look like at this place. If you read this text, you will get no information. Really? Is there no information? Is there a difference between this text and some nonsense like “Huardest gefburn”? Kjift – not at all! A blind text like this gives you

information about the selected font, how the letters are written and an impression of the look. This text should contain all letters of the alphabet and it should be written in of the original language. There is no need for special content, but the length of words should match the language.

Bibliography

[1] J. C. Dunlap, J. J. Loros, and P. J. DeCoursey, *Chronobiology: Biological Timekeeping*. Sinauer Associates, Inc., 2009.

[2] E. V. McCarthy, J. E. Baggs, J. M. Geskes, J. B. Hogenesch, and C. B. Green, "Generation of a novel allelic series of cryptochrome mutants via mutagenesis reveals residues involved in protein-protein interaction and CRY2-specific repression," *Mol. Cell. Biol.*, vol. 29, pp. 5465–76, Oct. 2009.

[3] G. T. van der Horst, M. Muijtjens, K. Kobayashi, R. Takano, S. Kanno, M. Takao, J. de Wit, A. Verkerk, A. P. Eker, D. van Leenen, R. Buijs, D. Bootsma, J. H. Hoeijmakers, and A. Yasui, "Mammalian Cry1 and Cry2 are essential for maintenance of circadian rhythms," *Nature*, vol. 398, pp. 627–30, Apr. 1999.

[4] E. E. Zhang, A. C. Liu, T. Hirota, L. J. Miraglia, G. Welch, P. Y. Pongsawakul, X. Liu, A. Atwood, J. W. Huss, J. Janes, A. I. Su, J. B. Hogenesch, and S. A. Kay, "A genome-wide RNAi screen for modifiers of the circadian clock in human cells," *Cell*, vol. 139, no. 1, pp. 199–210, 2009.

[5] K. Miyazaki, M. Mesaki, and N. Ishida, "Nuclear entry mechanism of rat PER2 (rPER2): role of rPER2 in nuclear localization of CRY protein.," *Mol. Cell. Biol.*, vol. 21, pp. 6651–9, Oct. 2001.

[6] C. H. Ko and J. S. Takahashi, "Molecular components of the mammalian circadian clock.," *Hum. Mol. Genet.*, vol. 15, pp. R271–7, Oct. 2006.

[7] K. Kume, M. J. Zylka, S. Sriram, L. P. Shearman, D. R. Weaver, X. Jin, E. S. Maywood, M. H. Hastings, and S. M. Reppert, "mCRY1 and mCRY2 are essential components of the negative limb of the circadian clock feedback loop," *Cell*, vol. 98, no. 2, pp. 193–205, 1999.

[8] J.-C. Leloup and A. Goldbeter, "Toward a detailed computational model for the mammalian circadian clock.," *Proc. Natl. Acad. Sci. U. S. A.*, vol. 100, pp. 7051–6, June 2003.

[9] H. P. Mirsky, A. C. Liu, D. K. Welsh, S. A. Kay, and F. J. Doyle, "A model of the cell-autonomous mammalian circadian clock.," *Proc. Natl. Acad. Sci. U. S. A.*, vol. 106, pp. 11107–12, July 2009.

[10] D. B. Forger and C. S. Peskin, "A detailed predictive model of the mammalian circadian clock," *Proc. Natl. Acad. Sci. U. S. A.*, vol. 100, pp. 14806–11, Dec. 2003.

[11] C. Lee, J.-P. Etchegaray, F. R. Cagampang, A. S. I. Loudon, and S. M. Reppert, "Posttranslational mechanisms regulate the mammalian circadian clock," *Cell*, vol. 107, pp. 855–67, Dec. 2001.

[12] Y. Lee, R. Chen, H.-m. Lee, and C. Lee, "Stoichiometric relationship among clock proteins determines robustness of circadian rhythms.," *J. Biol. Chem.*, vol. 286, pp. 7033–42, Mar. 2011.

[13] N. A. Cookson, L. S. Tsimring, and J. Hasty, "The pedestrian watchmaker: genetic clocks from engineered oscillators," *FEBS Lett.*, vol. 583, pp. 3931–7, Dec. 2009.

[14] N. Kurabayashi, T. Hirota, M. Sakai, K. Sanada, and Y. Fukada, "DYRK1A and glycogen synthase kinase 3beta, a dual-kinase mechanism directing proteasomal degradation of CRY2 for circadian timekeeping," *Mol. Cell. Biol.*, vol. 30, pp. 1757–68, Apr. 2010.

[15] E. Vielhaber, E. Eide, A. Rivers, Z.-H. Gao, and D. M. Virshup, "Nuclear Entry of the Circadian Regulator mPER1 Is Controlled by Mammalian Casein Kinase Ie," *Mol. Cell. Biol.*, vol. 20, pp. 4888–4899, July 2000.

[16] E. A. Griffin Jr., D. Staknis, and C. J. Weitz, "Light-Independent Role of CRY1 and CRY2 in the Mammalian Circadian Clock," *Science*, vol. 286, pp. 768–771, Oct. 1999.

[17] J. Andersson, B. Houska, and M. Diehl, "Towards a Computer Algebra System with Automatic Differentiation for use with Object-Oriented modelling languages," *3rd Int. Work. Equation-Based Object-Oriented Model. Lang. Tools*, pp. 99–105, 2010.

[18] A. C. Hindmarsh, P. N. Brown, K. E. Grant, S. L. Lee, R. Serban, D. A. N. E. Shumaker, and C. S. Woodward, "SUNDIALS : Suite of Nonlinear and Differential / Algebraic Equation Solvers," *ACM Trans. Math. Softw.*, vol. 31, no. 3, pp. 363–396, 2005.

[19] A. K. Wilkins, B. Tidor, J. White, and P. I. Barton, "Sensitivity Analysis for Oscillating Dynamical Systems," *SIAM J. Sci. Comput.*, vol. 31, no. 4, p. 2706, 2009.

[20] A. Relógio, P. O. Westermark, T. Wallach, K. Schellenberg, A. Kramer, and H. Herzel, "Tuning the Mammalian Circadian Clock: Robust Synergy of Two Loops," *PLoS Comput. Biol.*, vol. 7, p. e1002309, Dec. 2011.

[21] A. C. Liu, D. K. Welsh, C. H. Ko, H. G. Tran, E. E. Zhang, A. A. Priest, E. D. Buhr, O. Singer, K. Meeker, I. M. Verma, F. J. Doyle, J. S. Takahashi, and S. A. Kay, "Intercellular coupling confers robustness against mutations in the SCN circadian clock network," *Cell*, vol. 129, pp. 605–16, May 2007.

[22] R. N. Gutenkunst, J. J. Waterfall, F. P. Casey, K. S. Brown, C. R. Myers, and J. P. Sethna, "Universally sloppy parameter sensitivities in systems biology models," *PLoS Comput. Biol.*, vol. 3, pp. 1871–78, Oct. 2007.

[23] D. B. Kell and J. D. Knowles, "The role of modeling in systems biology," in *Syst. Model. Cell. Biol. from concepts to nuts bolts* (Z. Szallasi, J. Stelling, and V. Periwal, eds.), pp. 3–18, Cambridge: MIT Press, 2006.

[24] A. Raue, C. Kreutz, T. Maiwald, J. Bachmann, M. Schilling, U. Klingmüller, and J. Timmer, "Structural and practical identifiability analysis of partially observed dynamical models by exploiting the profile likelihood.," *Bioinformatics*, vol. 25, pp. 1923–9, Aug. 2009.

[25] M. Nihtilä and J. Virkkunen, "Practical identifiability of growth and substrate consumption models.," *Biotechnol. Bioeng.*, vol. 19, pp. 1831–50, Dec. 1977.

[26] J. E. Jiménez-Hornero, I. M. Santos-Dueñas, and I. García-García, "Optimization of biotechnological processes. The acetic acid fermentation. Part II: Practical identifiability analysis and parameter estimation," *Biochem. Eng. J.*, vol. 45, pp. 7–21, June 2009.

[27] A. Holmberg, "On the practical identifiability of microbial growth models incorporating Michaelis-Menten type nonlinearities," *Math. Biosci.*, vol. 62, pp. 23–43, Nov. 1982.

[28] M. Joshi, A. Seidel-Morgenstern, and A. Kremling, "Exploiting the bootstrap method for quantifying parameter confidence intervals in dynamical systems," *Metab. Eng.*, vol. 8, pp. 447–55, Sept. 2006.

[29] A. Goldbeter and J. Keizer, *Biochemical Oscillations and Cellular Rhythms: The Molecular Bases of Periodic and Chaotic Behaviour*, vol. 51. Cambridge: Cambridge University Press, 1998.

[30] T. Hirota, J. W. Lee, P. C. St. John, M. Sawa, K. Iwaisako, T. Noguchi, P. Y. Pongsawakul, T. Sonntag, D. K. Welsh, D. A. Brenner, F. J. Doyle, P. G. Schultz, and S. A. Kay, "Identification of Small Molecule Activators of Cryptochrome.," *Science*, vol. 337, pp. 1094–1097, July 2012.

[31] F. J. Doyle, R. Gunawan, N. Bagheri, H. P. Mirsky, and T.-L. To, "Circadian rhythm: A natural, robust, multi-scale control system," *Comput. Chem. Eng.*, vol. 30, pp. 1700–1711, Sept. 2006.

[32] E. D. Herzog, "Neurons and networks in daily rhythms.," *Nat. Rev. Neurosci.*, vol. 8, pp. 790–802, Oct. 2007.

[33] M. E. Hughes, L. DiTacchio, K. R. Hayes, C. Vollmers, S. Pulivarthy, J. E. Baggs, S. Panda, and J. B. Hogenesch, "Harmonics of circadian gene transcription in mammals," *PLoS Genet.*, vol. 5, p. e1000442, Apr. 2009.

[34] T. Hirota, J. W. Lee, W. G. Lewis, E. E. Zhang, G. Breton, X. Liu, M. Garcia, E. C. Peters, J.-P. Etchegaray, D. Traver, P. G. Schultz, and S. A. Kay, "High-Throughput Chemical Screen Identifies a Novel Potent Modulator of Cellular Circadian Rhythms and Reveals CKIα as a Clock Regulatory Kinase," *PLoS Biol.*, vol. 8, p. e1000559, Dec. 2010.

[35] T. Hirota, W. G. Lewis, A. C. Liu, J. W. Lee, P. G. Schultz, and S. A. Kay, "A chemical biology approach reveals period shortening of the mammalian circadian clock by specific inhibition of GSK-3beta.," *Proc. Natl. Acad. Sci. U. S. A.*, vol. 105, pp. 20746–51, Dec. 2008.

[36] L. T. Biegler, *Nonlinear Programming: Concepts, Algorithms, and Applications to Chemical Processes*. SIAM, 2010.

[37] H. G. Bock, E. Kostina, and J. P. Schloder, "Numerical methods for parameter estimation in nonlinear differential algebraic equations," *GAMM Mitteilungen*, vol. 408, no. 2, pp. 376 – 408, 2007.

[38] C. A. Floudas, *Nonlinear and Mixed-Integer Optimization*. New York, New York, USA: Oxford University Press, 1995.

[39] A. Wachter and L. T. Biegler, "On the implementation of an interior-point filter line-search algorithm for large-scale nonlinear programming," *Math. Program.*, vol. 106, pp. 25–57, Apr. 2006.

[40] HSL, "A collection of Fortran codes for large scale scientific computation," 2011.

[41] E. Jones, T. Oliphant, and P. Peterson, "SciPy: Open Source Scientific Tools for Python," 2001.

[42] R. Serban and A. C. Hindmarsh, "CVODES: the Sensitivity-Enabled ODE Solver in SUNDIALS," in *Proc. IDETC/CIE 2005*, (Long Beach, CA), 2005.

[43] M. A. Kramer, H. Rabitz, and J. M. Calo, "Sensitivity analysis of oscillatory systems," *Appl. Math. Model.*, vol. 8, pp. 328–340, Oct. 1984.

[44] E. G. Bure and E. Rosenwasser, "The study of the sensitivity of oscillatory systems," *Autom. Remote Control*, vol. 7, pp. 1045–1052, 1974.

[45] D. E. Zak, G. E. Gonye, J. S. Schwaber, and F. J. Doyle, "Importance of input perturbations and stochastic gene expression in the reverse engineering of genetic regulatory networks: insights from an identifiability analysis of an in silico network.," *Genome Res.*, vol. 13, pp. 2396–405, Nov. 2003.

[46] J. Bass, "Circadian topology of metabolism.," *Nature*, vol. 491, pp. 348–56, Nov. 2012.

[47] Z. Chen, S.-H. Yoo, and J. S. Takahashi, "Small molecule modifiers of circadian clocks.," *Cell. Mol. Life Sci.*, vol. 70, pp. 2985–98, Aug. 2013.

[48] R. Ye, C. P. Selby, N. Ozturk, Y. Annayev, and A. Sancar, "Biochemical analysis of the canonical model for the mammalian circadian clock.," *J. Biol. Chem.*, vol. 286, pp. 25891–902, July 2011.

[49] K. Yagita, F. Tamanini, M. Yasuda, J. H. J. Hoeijmakers, G. T. J. van der Horst, and H. Okamura, "Nucleocytoplasmic shuttling and mCRY-dependent inhibition of ubiquitylation of the mPER2 clock protein.," *EMBO J.*, vol. 21, pp. 1301–14, Mar. 2002.

[50] J. S. Takahashi, H.-K. Hong, C. H. Ko, and E. L. McDearmon, "The genetics of mammalian circadian order and disorder: implications for physiology and disease.," *Nat. Rev. Genet.*, vol. 9, pp. 764–75, Oct. 2008.

[51] S. Reischl, K. Vanselow, P. l. O. Westermark, N. Thierfelder, B. Maier, H. Herzel, and A. Kramer, "Beta-TrCP1-mediated degradation of PERIOD2 is essential for circadian dynamics.," *J. Biol. Rhythms*, vol. 22, pp. 375–86, Oct. 2007.

[52] A. Takano, Y. Isojima, and K. Nagai, "Identification of mPer1 phosphorylation sites responsible for the nuclear entry.," *J. Biol. Chem.*, vol. 279, pp. 32578–85, July 2004.

[53] L. Busino, F. Bassermann, A. Maiolica, C. Lee, P. M. Nolan, S. I. H. Godinho, G. F. Draetta, and M. Pagano, "SCFFbxl3 controls the oscillation of the circadian clock by directing the degradation of cryptochrome proteins.," *Science*, vol. 316, pp. 900–4, May 2007.

[54] S. I. H. Godinho, E. S. Maywood, L. Shaw, V. Tucci, A. R. Barnard, L. Busino, M. Pagano, R. Kendall, M. M. Quwailid, M. R. Romero, J. O'neill, J. E. Chesham, D. Brooker, Z. Lalanne, M. H. Hastings, and P. M. Nolan, "The after-hours mutant reveals a role for Fbxl3 in determining mammalian circadian period.," *Science*, vol. 316, pp. 897–900, May 2007.

[55] S. M. Siepka, S.-H. Yoo, J. Park, W. Song, V. Kumar, Y. Hu, C. Lee, and J. S. Takahashi, "Circadian mutant Overtime reveals F-box protein FBXL3 regulation of cryptochrome and period gene expression.," *Cell*, vol. 129, pp. 1011–23, June 2007.

[56] Y. Lee and E.-K. Kim, "AMP-activated protein kinase as a key molecular link between metabolism and clockwork.," *Exp. Mol. Med.*, vol. 45, p. e33, Jan. 2013.

[57] M. Gallego, E. J. Eide, M. F. Woolf, D. M. Virshup, and D. B. Forger, "An opposite role for tau in circadian rhythms revealed by mathematical modeling.," *Proc. Natl. Acad. Sci. U. S. A.*, vol. 103, pp. 10618–23, July 2006.

[58] E. S. Maywood, J. E. Chesham, Q.-J. Meng, P. M. Nolan, A. S. I. Loudon, and M. H. Hastings, "Tuning the period of the mammalian circadian clock: additive and independent effects of CK1ϵTau and Fbxl3Afh mutations on mouse circadian behavior and molecular pacemaking," *J. Neurosci.*, vol. 31, pp. 1539–44, Jan. 2011.

[59] K. Vanselow, J. T. Vanselow, P. l. O. Westermark, S. Reischl, B. Maier, T. Korte, A. Herrmann, H. Herzel, A. Schlosser, and A. Kramer, "Differential effects of PER2 phosphorylation: molecular basis for the human familial advanced sleep phase syndrome (FASPS)," *Genes Dev.*, vol. 20, pp. 2660–72, Oct. 2006.

[60] P. C. St. John and F. J. Doyle, "Estimating confidence intervals in predicted responses for oscillatory biological models.," *BMC Syst. Biol.*, vol. 7, p. 71, July 2013.

[61] R. Gunawan and F. J. Doyle, "Isochron-based phase response analysis of circadian rhythms.," *Biophys. J.*, vol. 91, pp. 2131–41, Sept. 2006.

[62] K. Ohsaki, K. Oishi, Y. Kozono, K. Nakayama, K. I. Nakayama, and N. Ishida, "The role of beta-TrCP1 and beta-TrCP2 in circadian rhythm generation by mediating degradation of clock protein PER2.," *J. Biochem.*, vol. 144, pp. 609–18, Nov. 2008.

[63] H. Lee, R. Chen, Y. Lee, S. Yoo, and C. Lee, "Essential roles of CKIdelta and CKIepsilon in the mammalian circadian clock.," *Proc. Natl. Acad. Sci. U. S. A.*, vol. 106, pp. 21359–64, Dec. 2009.